Mathematical Modeling of a Two-Phase Bubble-Column Reactor for Biodiesel Production from Alternative Feedstocks

A Thesis

Submitted to the Faculty

of

Drexel University

by

Minhazuddin Mohammed

in partial fulfillment of the

requirements for the degree

of

Master of Science

in

Chemical Engineering

March 2011

Dedication

Dedicated to my late grandfather Hasmat Ali who always believed in me

And, to our green Earth and her children for their well-being

Acknowledgments

I am sincerely grateful to my professor Dr. Richard A. Cairncross for his support and intellectual guidance during the course of this research. His passion for environment and sustainability combined with his stellar accomplishments in the field has constantly inspired and reminded me of the genuine philosophy of being a chemical engineer and researcher which is to have a purpose of serving our planet and its people.

Thanks to my research partner and friend Cory Melick (B.S. Chemical Engineering 2010, Drexel University) for his experimental work at the lab. His results were important for the validation of the work presented in this thesis. I highly appreciate his effort and contribution in producing the experimental results. I want to extend my gratitude to the entire current and past biodiesel research team for our discussions and their inputs in improving the biodiesel work in progress. I would like to thank EPA (P3 Design Award: SU-83352401) for their funding of the biodiesel research which facilitated the experimental work in the lab.

I want to thank the members of the approval committee – Dr. Nicholas Cernansky and Dr. Kenneth Lau for their invaluable feedback on the thesis. I owe my deepest gratitude to Dr. Giuseppe Palmese for his constant reminder to believe in myself. I am grateful to my academic advisors Professor Stephen Meyer and Dr. Cameron Abrams for being extremely supportive in finishing my work. I also thank Dr. Masoud Soroush for his process modeling coursework which provided me the knowledge of mathematical modeling.

Finally, I am thankful to my parents, my younger sister and my entire family for their encouragement. I sincerely thank the Banning family, Vanessa Sonntag and Priyadarshi Rishiraj for being there with me during both happy and tough times. I highly acknowledge the moral support from my friends Apoorv Chopra and Vimal Menon. My thanks are extended to my great cohort Iftekhar Ahmed who inspires me at all times. And lastly, I am grateful to my best friends Salvatore & Claudia Sansone for their unselfish support.

Table of Contents

List of Tables vi
List of Figures vii
Abstract x
1. Introduction and Background 1
1.1. Introduction 1
1.2. Background 4
1.2.1. 1st Generation Biodiesel Production Technology 4
1.2.2. 2nd Generation Biodiesel Production Technology 7
1.2.3. Process Intensification 9
1.2.4. Bubble Reactor Technology for Biodiesel Production 10
1.3. Thesis Objectives 16
1.4. Impacts/Motivation of Bubble Column Reactor (BCR) Model 17
2. Experimental Study of Biodiesel Production using Bubble Reactor Technology 18
2.1. Introduction to Prior Work 18
2.2. Results and Analyses 20
2.2.1. Effect of Temperature: 20
2.2.2. Effect of Catalyst: 21
2.2.3. Effect of Alcohol Feed Quality: 22
2.2.4. Effect of Alcohol Type: 24
2.3. Summary of Experimental Trends 25
2.4. Development and Evolution of Laboratory Bubble Column Reactor Prototypes 25
3. Bubble Column Reactor Semi-Batch Transient Model 28
3.1. Introduction 28
3.2. Description of Continuous Bubble Column Reactor (CBCR) Dynamic Model 28
3.2.1. Compartmentalization of Vapor-Liquid System 29
3.2.2. Gas-Liquid Mass Transport 31
3.2.3. Liquid Phase Reversible Reaction Kinetics 32
3.2.4. Equilibrium Limitations 33
3.2.5. Development of Reactor Model 34

3.2.6. Nondimensionalization of Reactor Model 38
3.3. Description of Model Parameters 40
3.4. Numerical Algorithm and Simulation Procedure: 43
3.5. Parameter Estimation & Model Validation 44
3.6. Results & Analyses 46
3.6.1. Introduction 46
3.6.2. Parameter Estimation & Model Validation 47
3.6.3. Typical Predictions of Semi-Batch Model 50
3.6.4. Robustness Study – Effect of Methanol Vapor Feed Quality 51
3.6.5. Effect of Reaction 53
3.6.6. Parametric Study of Characteristic Absorption Time Scale 54
3.6.7. Effect of Methanol Supply Rate 58
4. Bubble Column CSTR Steady State Model 60
4.1. Introduction 60
4.2. Description of Bubble Column CSTR Steady State Model 60
4.2.1. Single Stage Bubble Column CSTR 60
4.2.2. Multi Stage Bubble Column CSTR 61
4.3. Solution Procedure 64
4.4. Results and Analyses 65
4.4.1. Effect of Residence Time and Staging 65
4.4.2. Effect of Methanol Vapor Feed Quality 67
5. Conclusion & Future Directions 69
5.1. Concluding Discussion 69
5.2. Future Directions 70
Bibliography 72

List of Tables

Table 1: Average biodiesel emissions compared to conventional diesel..... 3

Table 2: Typical FFA content of natural oils and waste oils. 7

Table 3: Vapor phase steady-state BCR model for methanol and water..... 35

Table 4: Liquid phase dynamic bubble column reactor model..... 37

Table 5: Reduced form of liquid phase dynamic bubble column reactor model 39

Table 6: List of model parameters and their definitions..... 40

Table 7: List of parameters and values obtained during regression analysis of dynamic model with semi-batch experiments..... 47

Table 8: List of values for characteristic absorption time scales and Damköhler Number indicating three different operating regimes used in parametric sensitivity study of the dynamic CBCR model..... 55

Table 9: Design equations for multistage steady state continuous bubble column reactor 61

Table 10: List of the values of model parameters and reactor inlet conditions used for steady state modeling of bubble column reactor 64

List of Figures

Figure 1: Transesterification of triglycerides (TG) from plant and animal fats in presence of a base catalyst is the traditional route to produce biodiesel *5*

Figure 2: Saponification takes place as an undesired side reaction during base catalysis of triglycerides which reduces final biodiesel quality *6*

Figure 3: Esterification of free fatty acid (FFA) from plant and animal fats produce biodiesel (FAME) in presence of an acid catalyst. It is also accompanied by water production which retards the forward reaction. *8*

Figure 4: Schematic of absorption of methanol and desorption of water in bubble reactor technology during biodiesel reactions in oil *10*

Figure 5: Schematic of mass transfer of methanol and water in the presence of reversible esterification reaction inside a gas-liquid bubble column reactor used for biodiesel production *11*

Figure 6: Simplified schematic of the lab set-up of batch bubble reactor for biodiesel production. A, B, C and D represent the ports for methanol injection, stirrer, sample collection and thermometer respectively. Temperature was controlled using a hot oil bath or heating element (E) set at the desired reaction temperature. Methanol flow rate was controlled using a pump (F). Methanol vaporizes (X) as it enters the heated oil batch .. *19*

Figure 7: Reaction profiles of acid catalyzed homogenous esterification of oleic acid with methanol under different temperatures in semi-batch conditions *21*

Figure 8: Reaction profiles of different esterification catalysis of oleic acid in a bubble reactor with methanol *22*

Figure 9: Reaction profiles of oleic acid esterification in a bubble reactor fed with varying water content in methanol vapor feed. *23*

Figure 10: Reaction profiles of oleic acid esterification in a bubble reactor fed with varying water content in ethanol vapor feed *24*

Figure 11: (a) Teflon baffles with holes (b) Impellers pitched at 30° and 90° *26*

Figure 12: Evolution of bubble reactors (a) → (d) in laboratory. (a) Four-necked round bottomed flask as a semi-batch bubble reactor (b) 1st prototype of lab bubble column reactor (BCR) built in 2008 (c) 2nd prototype of BCR with improved design changes built in 2009 (d) acrylic reactor for visualization studies of baffling impacts. *27*

Figure 13: Schematic of compartment model showing important process mechanics inside a continuous bubble column reactor (CBCR) used for transient modeling of biodiesel production. *30*

Figure 14: Conceptual schematic of concentration profile in a gas-liquid system. 31

Figure 15: Quality of fit for parameter estimation based on experimental measurements of biodiesel conversion. Solid lines and dashed lines represent model predictions at 0% and 20% water content in vapor feed respectively. Squared markers and triangle markers represent experimental data from semi-batch experiments at 0% and 20% water content in vapor feed respectively. 49

Figure 16: Typical model predictions of concentration profiles of FFA, FAME, methanol and water in liquid phase compared with semi-batch experimental data for pure methanol feed (0% water content) at 120°C and 1 atm. 51

Figure 17: Model predictions of conversion profiles compared with semi-batch experimental data showing impact of varying water content as an impurity in methanol feed on biodiesel yield 52

Figure 18: Primary y-axis shows model predictions of methanol saturation profile in the presence (dashed lines) and absence (dotted lines) of reaction for different levels of methanol feed purity (0%, 10% and 20% respectively). Secondary axis shows model predictions for rate of reaction (continuous lines) along the reaction profile for three different levels of methanol feed purity (0%, 10% and 20% respectively). 54

Figure 19: Model predictions of concentration profiles and reaction rates from parametric sensitivity study by varying absorption time scale $\boldsymbol{\tau_A}$ for both pure methanol (a, c, e, g) and 80% impure methanol (b, d, f, h) feed conditions. $\boldsymbol{\tau_A}$ was varied in three different ranges of magnitude: (0.01h and 0.03h), (0.11h and 0.31h) and (1.01h and 3.01h) 57

Figure 20: (a) Model predictions and experimental biodiesel conversion profile for two different low (0.9 and 0.7 mL/h) and high (1.7 mL/h) vapor feed rates. Lines represent model predictions while markers represent experimental data. (b) On the primary axis model predictions for concentration profiles of methanol and water has been plotted while on secondary axis reaction rate is plotted. Continuous lines represent reaction rate, dashed and dotted lines represent methanol and water saturation respectively. 59

Figure 21: Steady state multistage bubble column reactor model in continuous mode as a cascade of 'n' CSTRs connected in series incorporating cross flow pattern 63

Figure 22: Different configurations of multistage BCRs connected in series exhibiting cross-flow pattern 63

Figure 23: Steady state bubble column reactor model predictions of conversion profiles for different multistage reactor configurations at (a) pure methanol vapor feed, and (b) impure methanol vapor feed with 20% water content 66

Figure 24: Effect of diminishing returns of number of stages on total residence time required to achieve >90% conversion in a continuous multistage bubble-column reactor operating at steady state *67*

Figure 25: Model predictions for conversion profiles at different methanol vapor feed quality for semi-batch model and different steady state multistage configurations of bubble column reactor *68*

Abstract

Mathematical Modeling of a Two-Phase Bubble-Column Reactor for Biodiesel Production from Alternative Feedstocks

Minhazuddin Mohammed

Advisor: Richard A. Cairncross, Ph.D.

This thesis project explores the fundamental mechanisms that control biodiesel production performance in a gas-liquid bubble column reactor. A mathematical model of a biodiesel bubble-column reactor was developed that accounts for the fundamental mechanisms of mass transport, chemical reaction kinetics and chemical reaction equilibrium. This model was compared to experimental data from a semi-batch reactor to validate the model and determine some of the model parameters. The model contains several important parameters that including a characteristic absorption time scale and a characteristic reaction time scale, the ratio of which is a Damköhler number. The Damköhler number indicates whether the reactor is operating in a mass-transfer limited or reaction kinetics limited regime. It was found from model predictions that the reactor is operated under kinetics limited regime (low Da $\approx$ 0.03). Because the model predicts the equilibrium limitations of the reaction, the model also reproduced trends of decreasing conversion and increasing conversion times when water is present in the methanol vapor feed. A steady state formulation of the transient model was derived to approximate the behavior of a cross-flow, continuous bubble-column reactor. Multistage modeling results showed that semi-batch reactor performance could be approximated when more than six reactor stages are connected in series.

1. Introduction and Background

1.1. Introduction

Biodiesel constitutes one of the rapidly growing sectors in the renewable fuels and energy industry. According to US EIA in 2009, renewable energy provides 8 percent of the nation's total energy demand in which biofuels contribute for about 20 percent (*1*). Biodiesel contributed approximately 2.55% of the entire biofuel consumption in 2009 (*2*). United States was the second largest producers of biodiesel worldwide in 2009 with an annual production of 736.3 million gallons and it was projected to reach 745.5 million gallons in 2010 and 1.7 billion gallons in 2020 (*3*). Biodiesel industry is projected to add US$24 billion to the US economy between the years of 2005 to 2015, assuming that biodiesel production reaches 650 million gallons by 2015. Biodiesel will improve the US economy by creating a projected number of 39,100 jobs in all sectors of the economy. Improved economic activity will prevent approximately US$13.6 billion from being spent on foreign oil while increasing American security in energy sector (*4*). Additionally, in the new Renewable Fuels Standard (RFS2), U.S. EPA (Environment Protection Agency) mandates a minimum of 1.15 billion gallons of bio-based fuels to be blended annually in US diesel fuel supplies by the end of 2010 compliance year (*5*). On December 17, 2010, the Obama administration revived the $1.00 per gallon federal tax credit on biodiesel which expired on December 31, 2009 (*6*). Clearly, in addition to ethanol, biodiesel is becoming the only competitive attractive choice as a bio-based liquid fuel for transportation and other diesel based sectors.

In addition to financial prospects, biodiesel is known for being a clean-burning diesel fuel with minimum negative environmental impacts and potential to greatly reduce greenhouse gas emissions. It is a biodegradable fuel with negligible sulfur content and ultra-low sulfur emissions. It has similar physical properties as fossil diesel fuel which makes it compatible for combustion in internal combustion (IC) engines and boilers (*7*). The exhaust emissions profile (see Table 1) and health related effects of biodiesel have been well documented in a technical report submitted to EPA under the Clean Air Act (CAA) Section 211(b) (*8*). Life cycle analysis of 100 percent biodiesel versus petroleum diesel shows that it virtually releases zero Carbon Dioxide (CO_2) to the atmosphere considering the entire CO_2 life cycle – cultivation, production of oil and conversion to biodiesel in plants (*9*). IC engines exhaust of 100 percent biodiesel show significant reduction in regulated pollutants such as carbon monoxide (48 percent), total unburned hydrocarbons (67 percent) and particulate matter (47 percent) as well as unregulated pollutants such as polycyclic aromatic hydrocarbons (PAHs) (80 percent) and nitrated PAHs (90 percent). A slight increase (on an average 10 percent) in NO_x compounds is observed in 100 percent biodiesel emissions of IC engines, but absence of sulfur in biodiesel allows to use NO_x control technologies and additives in biodiesel blends. These advantages make biodiesel a promising alternative fuel for use in current diesel engines without undergoing major design changes (*8*).

Table 1: Average biodiesel emissions compared to conventional diesel **(*10*)**

Emission Type	**B100**	**B20**
Regulated		
Total Unburned Hydrocarbons	-67%	-20%
Carbon Monoxide	-48%	-12%
Particulate Matter	-47%	-12%
NO_x	+10%	+2% to -2%
Non-regulated		
Sulfates	-100%	-20%*
PAHs (Polycyclic Aromatic Hydrocarbons)**	-80%	-13%
nPAHs (nitrated PAHs)**	-90%	-50%***
Ozone potential of speciated HC	-50%	-10%

*Estimated from B100
**Average reduction across all compounds measured
***2-nitrofluorine results were within test method variability

Positive economic projections from biofuel industry, federal and legislative mandates, increasing energy demands, depleting fossil fuel resources, growing concern/pressure to address the issues of global warming and pollution control are more than big reasons to increase biodiesel production and implement its usage at a full scale. Despite the merits of using biodiesel, there are challenges (technical, economic and political) which appear as roadblocks for our transition from fossil-fuel dependent nation to more balanced mix of renewable energy using country. The current biodiesel production technologies at the commercial scale, also known as first generation biofuel technologies, have been reported as a cause of recent increase in world prices for food and animal feeds (*11*). First generation biofuels technologies depend on vegetable oil derived from food crops or animal fats as the primary raw material which is a direct competition for availability of food resources in third world countries. As a result the feedstocks become more expensive and the total production costs (excluding government subsidies and grants) go higher which makes biodiesel (biofuels) an expensive option for energy security. To avoid political and ethical controversies, researchers and scientists have started to look

for alternative cheaper feedstocks (such as, agricultural and forest residues, non-food crops, trap grease) and accommodate the technical and economic challenges of biodiesel production by researching for new technologies. Biodiesel made from these feedstocks is known as second generation biodiesel and extensive investment is happening in both public and private sectors for R&D and near future deployment of new technologies at commercial level (*11*). It is likely that once the 2nd generation biodiesel production has been fully explored and secured, it will be chosen as a partial solution to the energy crisis in at least transportation sector due to its sustainability and environmental advantages.

1.2. Background

1.2.1. 1st Generation Biodiesel Production Technology

Monoalkyl ester derivatives of higher fatty acids are currently known as biodiesel. Biodiesel possesses physical properties similar to petroleum diesel, such as viscosity and cetane number. Compared to petroleum diesel biodiesel has a slightly higher cetane number which greatly eliminates knocking in engines ensuring smooth operation. Biodiesel has higher flash point which makes it safer to handle than petroleum diesel (*12*).

Existing biodiesel production technologies in industries primarily use homogeneous catalytic methanolysis of triglycerides in vegetable oils or animal fats to produce biodiesel. This conversion route known as transesterification reaction is usually carried out using a base catalyst (NaOH, KOH) at near ambient temperature (~40°C) and pressure ((*13*) (*14*) (*15*) (*16*)). According to the stoichiometry (Figure 1), three molecules

of alcohol (methanol) reacts with one molecule of triglyceride (TG) to produce three molecules of fatty acid methyl ester (FAME) also known as biodiesel and one molecule of glycerol.

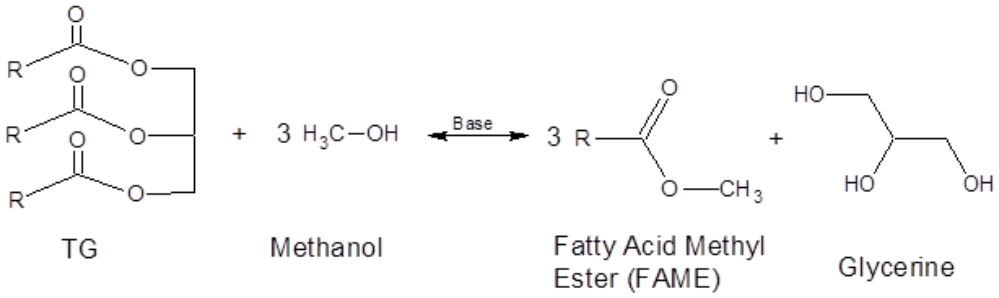

Figure 1: Transesterification of triglycerides (TG) from plant and animal fats in presence of a base catalyst is the traditional route to produce biodiesel **(*17*)**.

The above reaction occurs in three steps where in each step one alkyl chain of the glyceride molecule reacts to form one molecule of FAME. The reaction proceeds as: TG (triglyceride) → DG (diglyceride) → MG (monoglyceride) →G (glycerin) to form three molecules of FAME (*18*).

One of the several technical demerits associated with base catalysis is that the feedstock usually contains small amounts of free fatty acid (FFA) chains which participate in an undesirable side reaction known as saponification (Figure 2) ((*14*) (*19*) (*20*)). During saponification the metal ion head of the base catalyst replaces the proton attached to the carboxyl group of the fatty acid to form metal carboxylate derivative of FFA known as soap (*21*). Saponification is also associated with production of water which makes the process equilibrium limited if a major portion of the feedstock is free fatty acid. Van Gerpen reports that the reaction conversion falls by as much as 26% when the FFA content increases from less than 1% to about 7% (*14*).

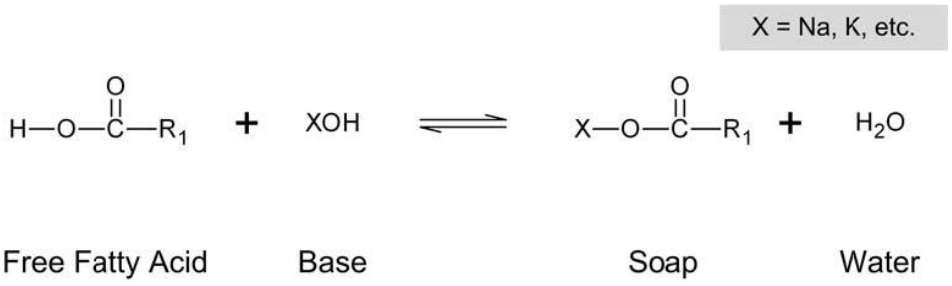

Figure 2: Saponification takes place as an undesired side reaction during base catalysis of triglycerides which reduces final biodiesel quality **(*22*)**

To address this issue, commercial technologies include a pre-treatment step before the reaction unit, where the feedstock is esterified with alcohol using a homogeneous acid catalyst (such as, H_2SO_4, H_3PO_4) to convert the FFA content of the feedstock into biodiesel before it reaches the transesterification step. This extra unit prevents the reaction step from being seriously hindered by saponification reaction while improving the final biodiesel quality and conversion (*23*) (*24*) (*25*). Although this two-step process improves biodiesel quality, an extra treatment unit combined with expensive feedstock makes biodiesel manufacturing an expensive process and also increases final biodiesel price. Other drawbacks of the current commercial technologies include high operating cost and energy consumption required for purification step and to recover excess alcohol and catalyst during downstream processing. Long reaction times, high alcohol to oil molar ratio and high catalyst concentration are also employed to address the mass transfer and equilibrium limitations of transesterification reaction. These steps also produce significant amount of toxic waste water at the time of downstream purification. Lower efficiency is incurred due to long residence times and long downstream processing time (*26*).

1.2.2. 2nd Generation Biodiesel Production Technology

Because of the many technical, ethical, political and economic challenges of 1st generation biodiesel production, much attention is drawn towards facilitating 2nd generation biodiesel production. These technologies are still in an R&D level and rely on cheaper feedstocks such as animal tallow, yellow grease, trap grease, forest residues and used fryer oil (*11*). The major advantages of using these feedstocks include but not limited to: (i) they do not compete with food resources such as corn or animal feedstocks for production of fuel (ii) they are non-toxic, sustainable and biodegradable (iii) they allow the process to recycle waste, and (iv) they reduce production costs (*27*). A major incompatibility in using these low quality feedstocks as a starting material for current commercial plants is that they contain a high percentage of free fatty acid which is not suitable for base catalyzed methanolysis due to soap formation (Table 1).

Table 2: Typical FFA content of natural oils and waste oils (**(*13*) (*23*) (*25*) (*28*) (*29*) (*30*) (*31*)**).

Low FFA Oil Sources	**FFA %**	**High FFA Oil Sources**	**FFA %**
Soybean Oil (crude)	0.3-0.7%	Mahua Tree	19%
Canola (crude)	0.3-1.2%	Jatropha tree	15%
Coconut (crude)	3%	Rubber Seed	17%
Corn (crude)	0.3-1.7%	Chinese Tallow	5.5%
Peanut	0.6%	Yellow Grease	<15%
Palm	<7%	Brown Grease	>15%
Milk Fat & Butter	<6.3%	Trap Grease	>95%

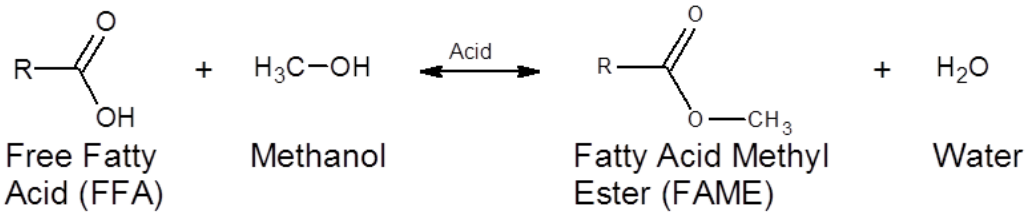

Figure 3: Esterification of free fatty acid (FFA) from plant and animal fats produce biodiesel (FAME) in presence of an acid catalyst. It is also accompanied by water production which retards the forward reaction.

An alternative route to biodiesel production is acid catalyzed esterification (Figure 3) of free fatty acids in presence of lower chain alcohols at a varying range of temperature starting from 60°C (*32*) (*33*) to 130°C (*34*). The acid catalysts usually chosen are homogeneous Bronsted acids in nature such as sulfuric acid, phosphoric acid, trichloroacetic acid and methanesulfonic acid ((*33*) (*34*)). The main role of the acid is to protonate the doubly bonded oxygen atom in free fatty acid thus making the carbonyl carbon electrophilic. This electrophilic molecule is then attacked by nucleophilic end of the hydroxyl group in methanol to form an intermediate structure. Then the acid catalyst deprotonates this charged intermediate to form fatty acid methyl ester (*21*).

Using alternative feedstocks will require technologies that treat both triglycerides and FFA. If we look at the stoichiometry of the reaction, it produces equimolar amounts of water and biodiesel which drives the reverse reaction. This makes the overall reaction equilibrium limited. This issue is generally addressed by using excess amount of methanol, excess amount of catalyst or increasing the temperature and pressure. Also, acid catalyzed esterification is very slow with triglycerides and is difficult to accomplish at normal esterification temperatures (*30*). Acid catalyzed processes require catalyst neutralization and recovery as downstream processing units and require corrosion

resistant materials for process vessels and instruments (*22*). Regardless of the many sustainability benefits of 2nd generation technology, the conversion routes are still not feasible due to lack of proper understanding of feedstocks and development of energy crops. So attempts need to be made to break the technological and cost barriers to make 2nd generation biodiesel technologies fully adaptable (*11*).

1.2.3. Process Intensification

In order to improve production efficiency, cost effectiveness and overcome the technical limitations associated with biodiesel production technologies, process intensification is an attractive area of research which can lead to solutions for limitations in commercial level scale-up. Process intensification can be achieved by improving catalysis, mass, heat and momentum transport of the conversion routes via use of advanced materials, alternate reaction pathways or novel reactors and processes (*26*). Use of amidation reactions (*35*), use of immobilized lipase as catalysts in absence of organic solvent ((*36*) (*37*) (*38*) (*39*) (*40*)), use of heterogeneous catalysts such as Amberlyst-15 (*41*), calcium catalysts (*42*), $SnCl_2$ (*43*), KF/ZnO (*44*), MgO, calcined hydrotalcites (*45*) and zeolites (*46*) (*47*) and use of inert solvents (*48*) have been amongst the recent novel materials being used to improve biodiesel production. In addition several promising novel reactor technologies and process techniques are being explored to intensify transport between methanol and oil: two-step esterification followed by transesterification ((*23*) (*24*) (*25*)), reactive distillation ((*49*) (*50*) (*51*)), supercritical reactors ((*52*) (*53*) (*54*)), microstructured reactors ((*26*) (*55*) (*56*)), bubble reactors ((*57*) (*58*) (*59*) (*60*)), packed bed reactors (*61*), three phase bubble column reactors (*62*), microwave reactors,

oscillatory flow reactors, ultrasonic irradiation, cavitational reactors, spinning tube reactors, centrifugal contactors (*26*).

1.2.4. Bubble Reactor Technology for Biodiesel Production

Use of bubble reactor technology for biodiesel production has been rarely explored in the literature so far. A bubble reactor has the potential for process intensification technique and significantly higher throughputs. In 2005, Kocsisova reported that feeding bubbling methanol into reactor and operating at temperatures higher than the boiling point of water at ambient pressure helps in simultaneous removal of water from oil phase produced during esterification (Figure 4) which improves final biodiesel conversion (*57*).

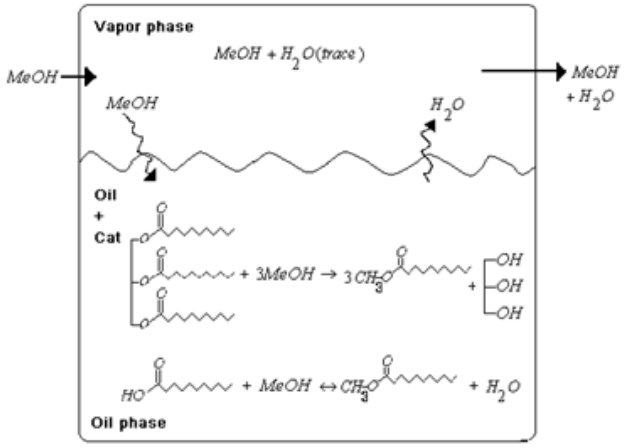

Figure 4: Schematic of absorption of methanol and desorption of water in bubble reactor technology during biodiesel reactions in oil

This advantage of in-situ water removal makes it an excellent alternative reaction technique to produce biodiesel from cheaper and low quality feedstocks with high free fatty acid content. Suwannakaran et al. (*62*) explored the feasibility of using mixed feedstocks (Glyceryl trioctanoate - TG and dodecanoic acid - FFA) for producing

biodiesel in presence of solid catalyst (calcined tungstated zirconia) via bubble reactor technology at elevated temperatures (130°C). They achieved 85% of FFA conversion and 22% of TG conversion within 2h of reaction. The relatively lower conversion is due to the competition between both TG and FFA for initial protonation of their carboxylic functionality followed by nucleophillic attack by methanol producing biodiesel. Water (pK_a = 15.7) (*63*) competes with free fatty acid (pK_a = 5.02) (*64*) for protonation and the pK_a values indicate that conjugate base (OH^-) of water is stronger than of free fatty acid which leads to poisoning of the acid catalysts as they become inactive in presence of water. Due to the advantage of in-situ removal of by-product water from the system in a bubble column reactor via evaporation helps in elimination of the poisoning effect of water on the acid catalysts and driving esterification reaction in the liquid phase towards completion (Figure 5).

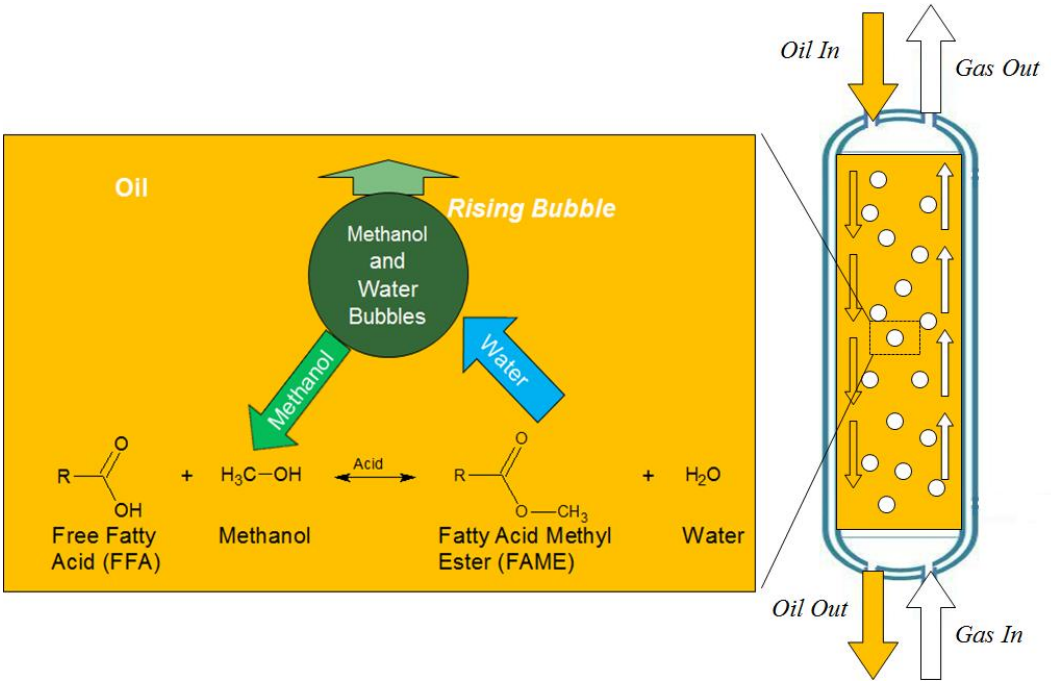

Figure 5: Schematic of mass transfer of methanol and water in the presence of reversible esterification reaction inside a gas-liquid bubble column reactor used for biodiesel production ***(17)***

At temperatures higher than boiling point of water, the reaction rate constant for esterification is two to three times higher than at the boiling temperature of methanol (*57*). Bubble reactor technology has also been used before at higher temperatures (250 – 290°C) using palm oil in the absence of a catalyst to predict its performance under a high methanol flow rate, but low conversion has been reported (maximum 60%) (*58*). In a later study, the same team observed a higher conversion (95%) at 290°C and also found that the rate constant of transesterification increases with increase in temperature (*59*).

In a bubble column reactor methanol bubbles rising through the reactor can provide required agitation to enable diffusion of methanol vapor into the oil phase for reaction (Figure 5). This will reduce the capital costs for mechanical agitation. A detailed study on performance of a discontinuous bubble column reactor for biodiesel production has been reported by Mollenhauer et al (*60*). In this paper the team reported process parameters by studying the mass transfer mechanism, hydrodynamic behavior of methanol bubbles and reaction kinetics in a non-mechanically agitated bubble column reactor operated at 80°C and 60°C. They reported biodiesel conversion of only 80% in 180 minutes when palm fatty acid distillate (acid value = 180) was used as the feedstock for FAME synthesis in the presence of an acid catalyst (*p*-toluene sulfonic acid) at 80°C. This could be due to the retarding effect from the presence of water in the system as the operating temperature was lower than the boiling point of water.

In summary bubble reactor technology can improve the economic feasibility of using a bubble column reactor for FAME production by reducing capital and operating costs for separation units (flash distillation and evaporators), purification units and reactor vessels. Combined with the prospective of using low quality feedstock as a raw materials, render

bubble columns as an attractive alternative 2nd generation technology for biodiesel production.

Bubble column reactors are generally known for their use in petrochemical, metallurgical, chemical and biochemical reactions. Their scaling up requires investigation and proper knowledge of multiphase fluid dynamic regimes inside the reactor, determining heat/mass transfer and kinetic parameters and establishing operating conditions. These studies are required to determine column design for scaling up and operate at optimum performance (*65*). Bubble reactor performance can be effectively investigated and measured by formulating quantitative models that interlinks the transport phenomena and kinetics inside the reactor. These models can be used for analyzing and characterizing operating regime of both semi-batch and continuous bubble column reactors. Conversion and concentration profiles can be measured and effect of process variables on them can be predicted. These studies are used for determining the final column design (such as, height to diameter ratio, operating conditions, number of stages for continuous reactors, necessity of reactor internals, etc.) and scale-up for manufacturing and correctly interpret data at R&D level (*66*). Validated bubble reactor dynamic models can also be used to design and control operation of processes using bubble column reactors.

1.2.5. Modeling of Biodiesel Processes

Several models have been published for biodiesel reactions and processes. The kinetic models of both esterification and transesterification reactions establish the order of the reaction, catalytic effect and the effect of temperature. Most acid catalyzed esterification kinetic models were pseudo-first order with respect to free fatty acid for the forward

reaction of esterification and second order for the reverse reaction (*32*). Alkaline transesterification of triglycerides has been observed to be pseudo-second order initially followed by a shift to first or zero order kinetics (*67*). Noureddini and Zhu (1997) (*18*) proposed and solved an extended kinetic model of Freedman et al. (*68*) for alkaline transesterification of soybean oil where they reported rate constants for two different agitation regimes (based on Reynold's number). They also fit the model based on second order kinetics with and without a shunt reaction scheme.

Kinetic mechanisms have been proposed in the context of producing biodiesel via process intensification. Immobilized enzyme catalysis models have been proposed and combined with experiments to estimate parameters and can be used to optimize and design scaled-up bioreactors for biodiesel production. A "Ping-Pong Bi Bi" mechanism for the kinetics of lipase enzymes with competitive reactant inhibition correctly describe the kinetics of transesterification of palm oil with methanol catalyzed by the lipase from *M. miehei* in *n*-hexane microaqueous system (*36*). The same model was lumped with mass transfer limitations in a dynamic model for transesterification to study biodiesel production from waste cooking oil. Mass transport and kinetic parameters were determined by comparison with experiments and the model was found to fit the data well. It led to find that methanol inhibits the reaction more than the triglyceride substrate (*37*). Cheirslip et al (2008) (*38*) developed three kinetic mechanisms and corresponding models for lipase catalyzed transesterification of palm oil fatty acids. The model was used to estimate parameters by fitting with experimental data. They found that the hydrolysis and ethanolysis proceeds simultaneously and that all the species affects the reaction rate.

Supercritical methanolysis and reactive distillation has proven useful in producing biodiesel. Kinetic mechanism has been proposed and models have been developed to explore the transesterification of triglycerides in the presence of supercritical methanol ((*52*), (*69*)). It was found that autocatalysis of fatty acids plays an important role in the two step process of FAME production via supercritical non-catalytic methanolysis and presence of water has a positive effect on formation of methyl esters due to hydrolysis of fatty acids under supercritical conditions which enhances the formation of FAME (*69*). Thermodynamic activity models such as UNIQUAC and UNIFAC available in commercial modeling software (Aspen) has been combined with liquid activity based kinetic models to study biodiesel production via reactive distillation. Damköhler Numbers were defined to capture the design elements of the reactive entrainer for biodiesel production from free fatty acids with higher alcohols (2-ethylhexanol) in the presence of sulphated zirconia catalyst (*49*), (*50*), (*51*).

Simulation studies have been done to compare reactor performances and cost of production using these kinetic models. Interstage separation has proved effective in both PFR and CSTR configurations to produce biodiesel. Two stage PFRs showed 15% higher yield in biodiesel produced via alkaline transesterification, than CSTRs with two interstage separations (*70*). Mjalli et al. (2009) first developed a full mechanistic process model of a transesterification reactor for biodiesel production and implemented it for an adaptive control system. The model included both dynamic mass and heat balances as well as a simplified lumped kinetic model but neglected any mass transfer limitations (*71*). Slinn and Kendall (2008) (*72*) used iterative mass transfer and reactor design equations to determine bubble size during biodiesel reaction. This was further used to

establish the kinetics of the reaction in the reactor. This is the first time a process model was used including both mass transfer and kinetic models to study the controlling action of both of these mechanisms during biodiesel reaction. They ignored any thermodynamic limitations during this study.

To our knowledge there are no mechanistic models in the literature for biodiesel production via bubble reactor technology. Thus far mechanistic and kinetic modeling has been extensively done in both traditional biodiesel technologies and process intensification technologies to establish or explore their technical and economic feasibility.

1.3. Thesis Objectives

The main objective of the research presented in this thesis is to develop a mathematical model of a bubble column reactor (BCR) for biodiesel production from low quality feedstock via acid catalyzed esterification using methanol. This model will account for the mass transfer limitations of methanol between oil and gas phase in a bubble column reactor due to its heterogeneous nature. It will account for the slow nature of the kinetics of esterification reaction and reaction equilibrium limitations that affect methanol transport between oil and vapor phase. It will be validated using experiments and used to predict reactor performance under different operating regimes. This will allow us to identify advantageous process conditions for full scale biodiesel production using BCR technology. This model will be used to explore the robustness of the BCR when subjected to varying quality of alcohol feed in terms of water content. A steady-state formulation of the model will be used to determine the performance of a continuous

single/multi “staged” bubble column reactor and its impacts on overall biodiesel conversion.

1.4. Impacts/Motivation of Bubble Column Reactor (BCR) Model

The exploratory work conducted in the Drexel Biofuels Research Laboratory on acid catalyzed biodiesel production via bubble reactor technology provided the motivation to develop a mathematical model which could further guide the design and operation of a bubble column reactor on a large scale. Based on the results from prior work, such a mechanistic model could be used to determine the feasibility of a scaled-up reactor by understanding the mechanics of transport/kinetics and operating limitations. The model contains many parameters that will help improve understanding of the key mechanisms controlling conversion to biodiesel. For example, the Damkohler Number scales the characteristic reaction and mass transfer rates. It is necessary to determine if the BCR performance is limited by the diffusion rate of methanol vapor into the oil phase or the actual rate of reaction between oil and methanol. Hence the model will help optimize the design of a scaled-up continuous BCR that can be implemented in a full scale biodiesel production process. To achieve this, the model will help in reducing the number of parametric experiments needed to be conducted on a large scale by estimating FFA conversion under different operating conditions.

2. Experimental Study of Biodiesel Production using Bubble Reactor Technology

2.1. Introduction to Prior Work

Several experiments have been conducted by Biodiesel Research Group in the Biofuels Laboratory of Drexel University under the supervision of Dr. Richard Cairncross to explore the impacts of different operating conditions on biodiesel production from refined trap grease in a bubble column reactor. These experiments were primarily conducted by Cory Melick (B.S. Chemical Engineering, 2010, Drexel University), along with few other researchers. The experiments can be categorized into several areas which established the technical feasibility of converting high FFA oils into biodiesel in a bubble column reactor. They included: effect of temperature on kinetics of FFA conversion to biodiesel, effect of using different classes of catalysts, effect of varying alcohol vapor flow rate, effect of using different types of alcohol and effect of purity of feed content.

The exploratory studies were conducted in several types of reactors under batch and semi-batch conditions. Majority of the initial studies were performed in four necked round bottomed flask sub-merged into an oil bath (see Figure 6 and 12a) and graduated cylinder as a semi-batch bubble column reactor. A thermometer was inserted into the reaction mixture to monitor the reaction temperature. Oil batch of oleic acid (amount changed according to the experiment) was initially charged into the reactor and heated until reaction temperature is achieved. The reaction temperature was maintained by keeping the reactor submerged in an oil bath or using a heating element. Catalyst was added to the mixture directly at the beginning of heat-up. The reaction mixture was

continuously agitated using motor-driven stirrer at a particular speed. Liquid alcohol was pumped into the bubble reactor continuously using a peristaltic pump or syringe pump over a length of time and flow rates were varied depending on the experiment as it vaporized before entering the reactor (Figure 6).

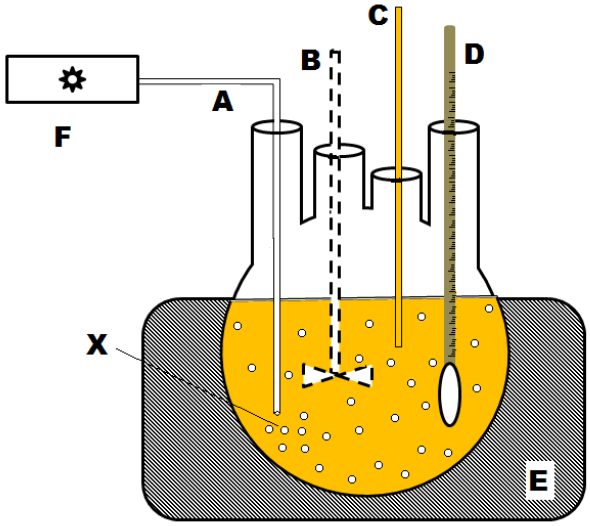

Figure 6: Simplified schematic of the lab set-up of batch bubble reactor for biodiesel production. A, B, C and D represent the ports for methanol injection, stirrer, sample collection and thermometer respectively. Temperature was controlled using a hot oil bath or heating element (E) set at the desired reaction temperature. Methanol flow rate was controlled using a pump (F). Methanol vaporizes (X) as it enters the heated oil batch **(*73*)**.

Titration was employed as the analytical method to measure biodiesel conversion of the collected samples from the experiments because oleic acid was used as raw material. Samples were collected at regular intervals from the reactor contents and titrated against a basic dilute solution of sodium hydroxide. Iso-propanol containing phenolphthalein was used to dilute the sample in order to avoid phase separation with water based titrant. This analytical method provided a way to calculate biodiesel conversion which is equal to the initial number of moles of oleic acid in the sample minus number of moles of residual acidity measured by titration; this difference is normalized by the initial number of moles

to get a fractional conversion. A number of modifications have been made to the reactor configuration to increase the mass transfer of methanol and water between the vapor and oil phases. Several alternative reactor designs are discussed below (Section 2.4).

2.2. Results and Analyses

2.2.1. Effect of Temperature:

Several temperature ranges were explored in semi-batch studies to establish the optimum operating range. 200 mL (176.8 g) of oleic acid was charged into the reactor and heated to the desired reaction temperature. Once the temperature is reached and stabilized, methanol was fed at 1.0 mL/min and sulfuric acid was added as a catalyst in the amount of 0.7% by weight of the oil (1.2 g). Samples were collected 5 minutes after the methanol was charged into the reactor.

From Figure 7 it can be seen that conversion profile plateaus at different values for three temperature regions. For experiments conducted at temperature below the boiling point of methanol (60°C), conversion progresses at slowest rate (~3 h) and levels off at approximately 60%. For temperature region between the boiling point of methanol and water, reaction proceeds faster and conversion profile levels off at a higher range of 90%. Fastest conversion is achieved within an hour when reaction is conducted at temperatures above the boiling point of water (> 100°C) and levels off between 95 percent and 100 percent. This conversion is in agreement with reported values in literature for studies conducted within similar temperature range (*57*).

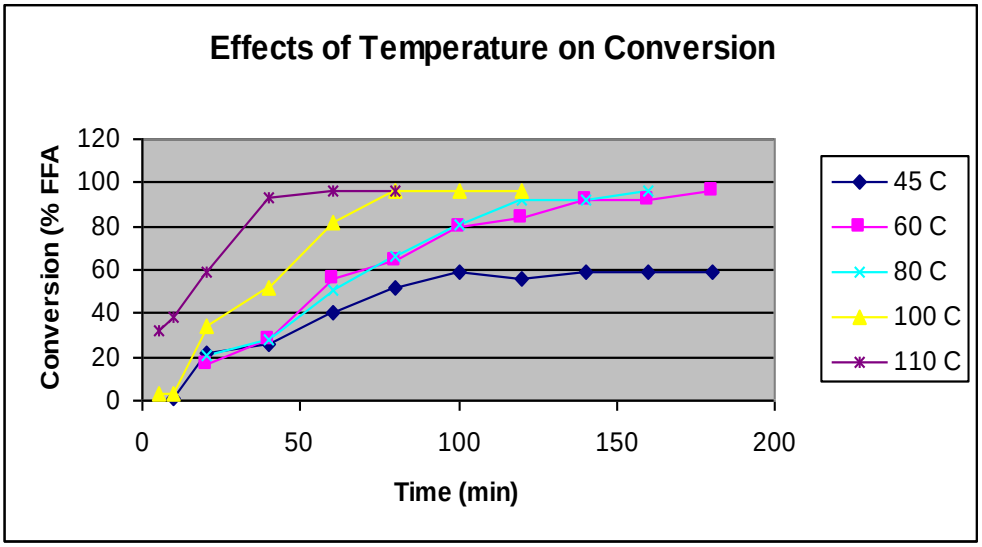

Figure 7: Reaction profiles of acid catalyzed homogenous esterification of oleic acid with methanol under different temperatures in semi-batch conditions **(*73*)**.

2.2.2. Effect of Catalyst:

Several catalysts were selected to explore catalyst effectiveness on biodiesel production from free fatty acids. 200 ml of oil (oleic acid) was reacted with methanol fed at 1 mL/min in the presence of three different catalysts: p-toluenesulfonic acid (PTSA), hydrochloric acid and sulfuric acid, while reaction temperature was maintained at 120°C. PTSA catalyst was prepared by absorbing it in sulfuric acid bath for 20 minutes followed by drying in air. 11.69 grams (6.6 wt% of oil) of PTSA and sulfuric acid in the amount of 0.7 wt% of oil was used to catalyze the reactions (*17*).

Figure 8 shows the reaction profiles for different catalysis of oleic acid with pure methanol. A net increase in conversion is observed for studies conducted with PTSA/H_2SO_4 compared to hydrochloric acid. Reaction rate of hydrochloric acid catalysis is much slower than for studies conducted using PTSA/sulfuric acid. A similar reaction profile is observed for reactions catalyzed by PTSA or sulfuric acid, where reaction

progresses faster and a high overall conversion between 95% and 100% is achieved in approximately 60 – 90 minutes. Hydrochloric acid (pK_a = -10.0 at 25°C) and sulfuric acid (pK_a = -3.0 at 25°C) are both strong acids but sulfuric acid is diprotic in nature due to which it releases more protons and facilitates production of electrophilic fatty acid chains in oil available for attack by nucleophilic methoxy radicals (*34*), (*63*). This result is in agreement with values reported before in literature for studies conducted in presence of similar catalysts ((*60*) (*57*)).

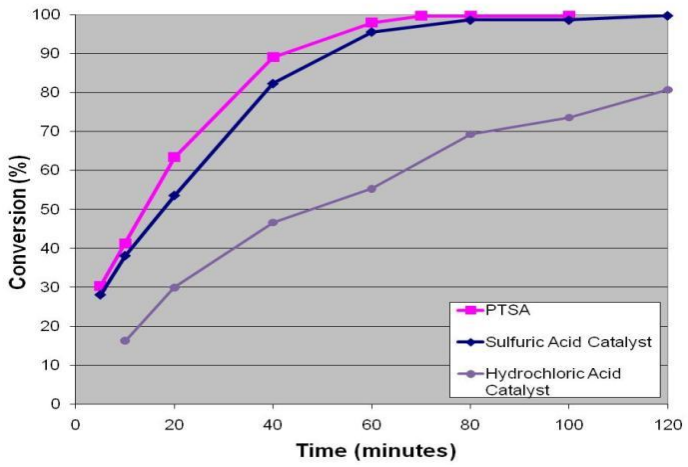

Figure 8: Reaction profiles of different esterification catalysis of oleic acid in a bubble reactor with methanol **(*73*)**.

2.2.3. Effect of Alcohol Feed Quality:

Several experiments were conducted to determine the impact of water content in alcohol feed on overall biodiesel conversion. Experiments were conducted under four different vapor feed conditions: pure methanol, 5%, 10% and 20% water content by volume of total vapor feed. Since water is a major byproduct of esterification reaction, it is known for its poisoning effect on the catalyst and makes the reaction equilibrium

limited which lowers the overall conversion (*57*). 70 ml of oil (oleic acid) was reacted at 120°C with methanol fed at 0.33 mL/min in the presence of sulfuric acid at 0.7% by weight of oleic acid. For these experiments, a graduated cylinder was used as a bubble column reactor.

In Figure 9 conversion profiles from bubble reactor studies show that the reaction rate is slowed by increasing the water content in the alcohol feed. Negligible drop in overall conversion (99% to 96%) and longer reaction time from 90 minutes to 120 minutes is observed, as water content increase from 0% to 20% in methanol feed. This indicates that high conversion is still attained in presence of water in vapor feed and that by-product water is vaporized during the course of reaction. Bubble reactor shows potential robust nature towards of being able to use lower and cheaper grade methanol vapor as feedstock.

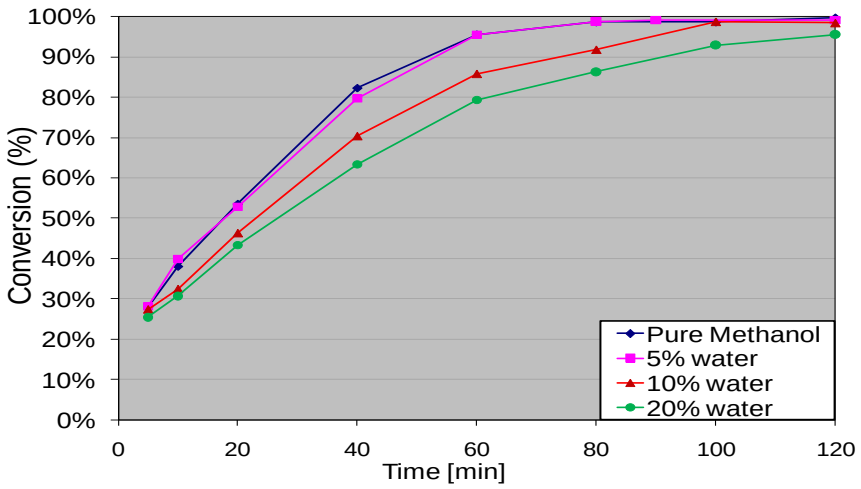

Figure 9: Reaction profiles of oleic acid esterification in a bubble reactor fed with varying water content in methanol vapor feed ***(73)***.

2.2.4. Effect of Alcohol Type:

Studies were performed to establish the feasibility of using ethanol as a raw material for biodiesel production. Ethanol can be derived from renewable resources which imply that fatty acid ethyl esters (FAEE) are of more renewable nature than FAME. 70 ml of oil (oleic acid) was reacted at 120°C in a graduated cylinder with ethanol fed at 0.33 mL/min in the presence of sulfuric acid at 0.7% by weight of oleic acid.

Figure 10 shows reaction profiles for studies conducted using ethanol and ethanol containing water as alcohol feed. In prior studies, ethanol generally reacts slower than methanol due to presence of steric hindrance (bigger molecule than methanol) during reaction and avoided for use in biodiesel production (*34*). However, in our results, the conversion profiles for pure methanol and pure ethanol feeds are nearly identical, and both produce a high overall conversion in less than 90 minutes. This shows that it is not necessary to break the ethanol-water azeotrope to use ethanol for biodiesel production.

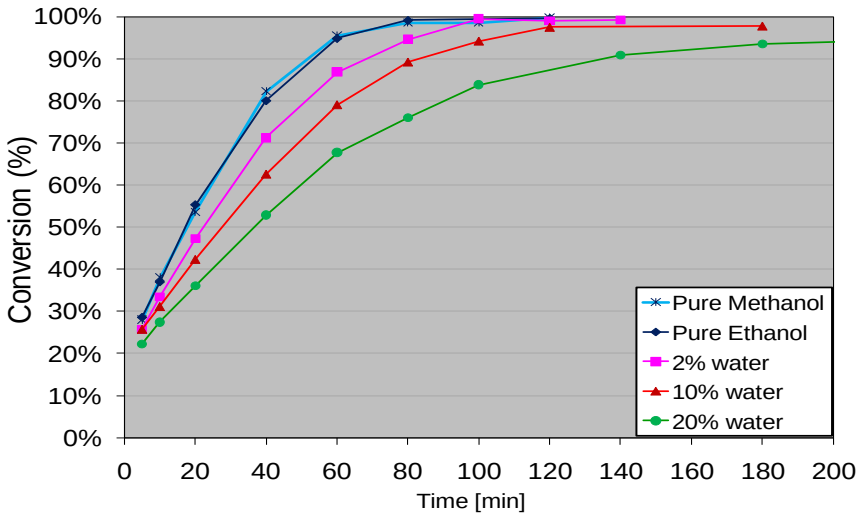

Figure 10: Reaction profiles of oleic acid esterification in a bubble reactor fed with varying water content in ethanol vapor feed ***(73)***.

2.3. Summary of Experimental Trends

From the above exploratory studies, we were able to establish few standard operating conditions for the bubble reactor. We observed that significant conversion is achieved when reaction temperature is kept above 120°C. Sulfuric acid is an effective catalyst to attain faster and higher overall conversion. We also saw that 0.7 percent by weight sulfuric acid in oleic acid is enough for high reaction rate. Both methanol and ethanol were effective in obtaining high biodiesel conversion. Impure alcohol feed slows down reaction progress but high overall conversion is still attainable within acceptable reaction times which indicated the robustness of the bubble reactor technology.

2.4. Development and Evolution of Laboratory Bubble Column Reactor Prototypes

Based on the semi-batch work in the lab, two prototypes of continuous bubble column reactors have been developed in our laboratory for biodiesel production by two successive mechanical engineering senior design teams in 2008 and 2009. The first reactor was developed by the 2008 MEM senior design team as a double pipe heat exchanger inside which oil and methanol flow in counter-current direction (Figure 12b). Methanol vapor forms bubbles after entering reactor gets dispersed uniformly across the cross-section of the column which provides the agitation required for achieving the desired conversion. It was designed for a maximum volume of 600 mL oleic acid. Methanol vapor is fed into the bottom using a small peristaltic pump. Fresh oil enters through the top of the reactor and is recirculated using a peristaltic pump. Converted oil in the form of biodiesel and unreacted oil is drawn from the bottom. The unreacted methanol along with byproduct water leaves the system in the form of vapor through the

top. A hot oil reservoir was used to pump heating fluid into the shell side of the reactor in order to maintain the reaction temperature (*74*).

Later the design was modified and a new bubble column reactor was constructed by the 2009 MEM senior design team (Figure 12c). In this design heating tape was wrapped around the reactor and covered with insulation. This reactor had provisions for adding agitator shaft through a hole on the top and removable top flange for installing baffles as reactor internals. This design was inspired via studies using an acrylic reactor (Figure 12d) to visualize the effects of baffles and agitation on methanol bubbles. Baffling was added with the intention to gain higher reaction rate and increase residence time. Baffling is also known to prevent backmixing in bubble column reactors under continuous mode. The baffles divide the column into stages where an ideal plug flow behavior or mixed behavior between plug flow and CSTR can be achieved via optimization of baffle design (*75*) (*76*). Increasing residence time will ensure that fresh oil coming through the top is not mixed with product biodiesel at the bottom when operated under continuous mode. Two types of baffles and agitators were designed – Teflon baffles (Figure 11a) with two different sizes of holes, blade impeller (30° pitched) and blade radial impeller (90° pitched) (Figure 11b) (*77*).

(a) (b)

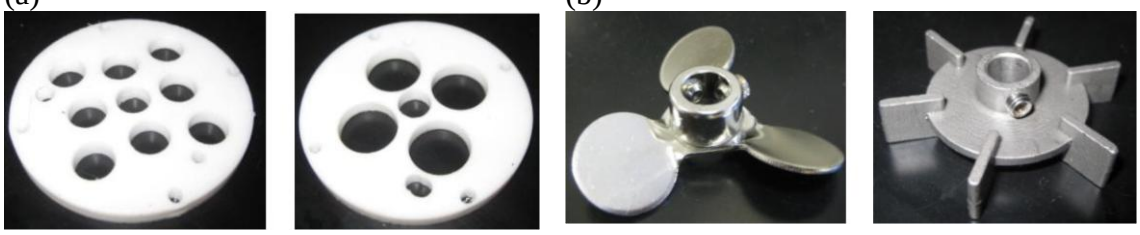

Figure 11: (a) Teflon baffles with holes (b) Impellers pitched at 30° and 90° **(*77*)**.

(a) (b)

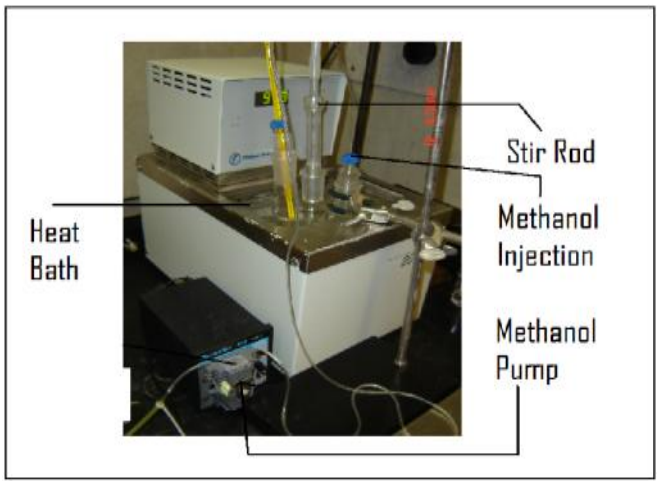

(c) (d)

Figure 12: Evolution of bubble reactors (a) → (d) in laboratory. (a) Four-necked round bottomed flask as a semi-batch bubble reactor (b) 1st prototype of lab bubble column reactor (BCR) built in 2008 (c) 2nd prototype of BCR with improved design changes built in 2009 (d) acrylic reactor for visualization studies of baffling impacts **(*17*)**.

3. Bubble Column Reactor Semi-Batch Transient Model

3.1. Introduction

Using bubble column reactors is a new strategy for process intensification of biodiesel production from alternative low quality feedstock. Performance of bubble column reactors in the context of biodiesel production has been rarely explored ((*58*), (*59*), (*57*), (*60*)) and no mechanistic modeling studies have been reported so far. In this current chapter, we derive a mechanistic model starting from the species mass balances in both phases (gas and liquid). The parameters in the final model are used to link the reactor performance with input variables and operating variables. This model can be used to optimize the operating conditions and determine scale up feasibility and reactor design. The reactor model is found to be valid for a range of reaction-diffusion modulus (Damköhler number) based on performance of the lab bubble reactor.

3.2. Description of Continuous Bubble Column Reactor (CBCR) Dynamic Model

The bubble column reactor model developed here is a transient model which approximately describes the mechanics of the mass transport, reversible kinetics of the reaction and the equilibrium limitations of the physical system. These three factors can narrow the operational regimes of the bubble column reactor and give rise to multiple steady states. The modeling was approached initially with several important assumptions for simplicity in modeling while capturing the most important physical mechanisms in a gas-liquid biodiesel producing bubble column reactor. This model adequately describes

the overall behavior of the bubble column reactor in production of biodiesel from free fatty acids.

3.2.1. Compartmentalization of Vapor-Liquid System

The heterogeneous physical system inside the bubble column reactor is compartmentalized into two parts to discretely address the mechanisms in each phase of the reactor. Vapor phase consists of methanol and water vapor while the liquid phase consists of oil, biodiesel, methanol, water and catalyst (sulfuric acid). An approximate compartment model is illustrated in Figure 13 where all the process and state variables are listed. For simplicity it is assumed that both phases are well mixed and there is no spatial concentration gradient inside the reactor. The flow rates of the feed and effluent are considered to be constant similar to an ideal CSTR configuration.

The system is isothermal, so any spatial or temporal gradient of temperature has been neglected. We invoked the assumption of constant molal overflow for both methanol and water (also known as equimolal overflow) inside the reactor for vapor phase modeling purposes, so any change in their flow rates should be caused by the feed and exit streams. Moreover, we assume constant flow rate of the vapor stream through the system, consequently we can perform pseudo-steady state molar balance on methanol and water in the vapor phase.

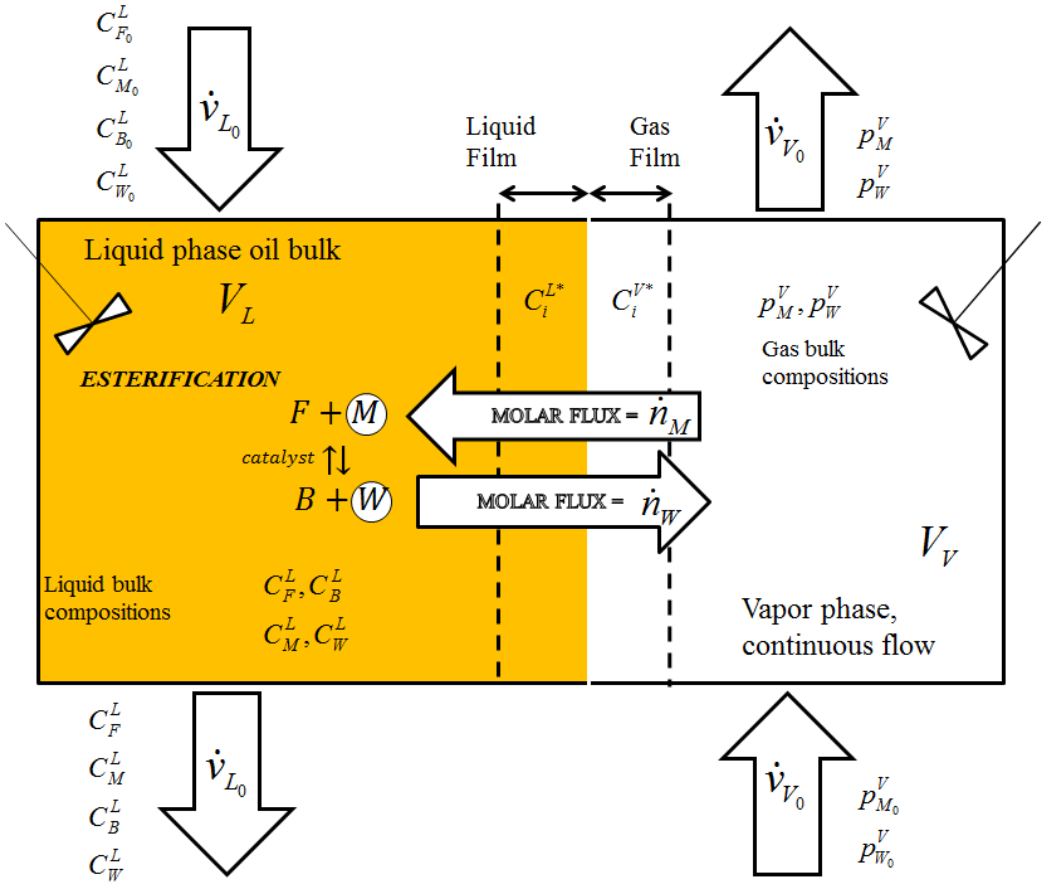

Figure 13: Schematic of compartment model showing important process mechanics inside a continuous bubble column reactor (CBCR) used for transient modeling of biodiesel production.

3.2.2. Gas-Liquid Mass Transport

In order to model the transport of methanol and water at the gas-liquid interface we consider that mass transport occurs across the two phases in both directions as methanol enters the system in vapor phase and is absorbed in the oil phase at high reactor temperature to react with the free fatty acid in oil phase. The reversible esterification reaction is assumed to occur only in the bulk liquid phase, because we consider high mass transfer resistance in liquid phase and negligible resistance in vapor side. Biodiesel is formed from the reaction with water as the side product which desorbs from the liquid phase in vapor form. Effective mass transfer coefficients for both water and methanol are assumed to be same for simplicity in modeling. In vapor phase, we assume that the mass transport of methanol and water at the interface are driven by partial pressure differences or concentration differences between the two phases (Figure 14).

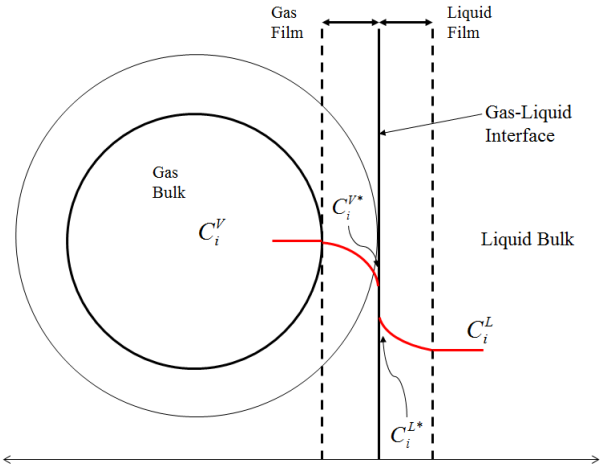

Figure 14: Conceptual schematic of concentration profile in a gas-liquid system.

For mass transfer from liquid to the vapor phase, Equation 1 shows the constitutive convective mass transport relationship used for the mass flux of methanol and water across the boundaries during modeling.

$$\dot{n}_{i,mt} = (ka)V_L\left(C_i^{V^*} - C_i^V\right) \quad [1]$$

Where, $\dot{n}_{i,mt}$ is molar flux of species 'i' between liquid and gas phases, 'ka' is the effective volumetric mass transfer coefficient based on gas-phase concentration of species *'i'* where 'i' refers to either chemical species methanol or water. $C_i^{V^*}$ is the hypothetical vapor concentration of species *'i'* that will be in equilibrium with its bulk concentration in liquid phase. This concentration determines the extent of absorption/desorption between the two phases. The above equation is based on the two-film model and using the modified Fick's law, describes a steady state mass flux, $\dot{n}_{i,mt}$, across the gas-liquid interface.

3.2.3. Liquid Phase Reversible Reaction Kinetics

Several transesterification and esterification kinetic models are available in literature where most of them assume the forward reaction is pseudo-first order with first order in fatty acid and zero order in methanol while the reverse reaction is second order with first order respect to water and biodiesel ((*32*), (*34*), (*78*)). In our work the kinetics of the esterification reaction is assumed to be elementary order in all reacting species and rate constants obey Arrhenius behavior. It is also reversible and equilibrium limited in nature. This is due to the fact that our experiments did not use high molar excess of methanol which may cause the kinetics to be dependent on methanol. Equation 2 and 3 shows the constitutive relationships used for the reaction kinetics and reaction equilibrium during modeling.

$$-r_F = -r_M = r_B = r_W = k_f C_F^L C_M^L - k_r C_B^L C_W^L \quad [2]$$

$$K_{eq} = \frac{k_f}{k_r} \quad [3]$$

Where, $'\pm r_i'$ refers to esterification reaction rate relative to species *'i'*, k_f and k_r are forward and reverse rate constants and 'K_{eq}' is the equilibrium constant. The overall reaction is considered to be exothermic which has not been taken into account in the current modeling task as we did not perform any modeling on energy balances.

3.2.4. Equilibrium Limitations

Both methanol and water are assumed dilute in oil phase which allows the use of Henry's law coefficients for relating concentrations between the phases and accounting for the solubility limitations of both species. Thermophysical properties of vapor phase such as solubility and density are considered to be function of temperature and pressure. The process operates at atmospheric pressure and constant temperature. Solubilites and Henry's coefficients are assumed constant over the range of concentrations and partial pressures. The Henry's law constants of both species for the given system are related to solubilities according to the following expression (Equation 4),

$$H_i = \frac{p_i^{V^*}}{C_i^L} \quad [4]$$

Where, H_i is the Henry's law coefficient of either methanol or water, C_i^L is the solubility of methanol or water and $p_i^{V^*}$ is the hypothetical partial pressure of methanol or water that would be in equilibrium with its concentration C_i^L in the liquid phase.

The density or concentration of the vapor phase is assumed to vary on the system pressure and temperature according to the ideal gas law given by Equation 5,

$$C_i^V = \frac{p_i^V}{RT} \quad [5]$$

3.2.5. Development of Reactor Model

The complete description of the bubble column reactor includes a set of mass conservation equations for each species in liquid phase and vapor phase. The generalized mass balance law for each component can be given as:

$$\text{Accumulation} = \begin{pmatrix}\text{Flow In -}\\ \text{Flow Out}\end{pmatrix} + \begin{pmatrix}\text{Generation or}\\ \text{Consumption}\\ \text{by reaction}\end{pmatrix} - \begin{pmatrix}\text{Interphase}\\ \text{Mass Transfer}\end{pmatrix} \quad [6]$$

Vapor Phase Modeling: In vapor-phase of the bubble column reactor, there are no reactions and the mass balance equations are assumed to be steady state. Under steady state conditions and substituting equation 1 for interphase mass transfer term we can write the vapor phase model as follows,

$$0 = \dot{v}_{V_0} C_{i_0}^V - \dot{v}_{V_0} C_i^V + (ka) V_L \left(C_i^{V^*} - C_i^V\right) \quad [7]$$

Where, C_i^V and $C_{i_0}^V$ are the vapor phase concentrations of either methanol or water *('i')* in bulk and vapor feed. $\dot{v}_{V_0}$ is the vapor feed rate which remain constant and also the outlet vapor flow rate.

Vapor phase molar concentrations can be substituted via ideal gas law (equation 5) to change into partial pressures and equation 7 can be rewritten as,

$$\frac{\dot{v}_{V_0}}{RT}\left(p_{i_0}^V - p_i^V\right) = \frac{(ka)V_L}{RT}\left(p_i^V - p_i^{V^*}\right)$$

Henry's Law (Equation 4) is used to relate the solubility and $\left(p_i^{V^*}\right)$. So the above balance can rewritten as,

$$\dot{v}_{V_0}\left(p_{i_0}^V - p_i^V\right) = (ka)V_L(p_i^V - H_i C_i^L)$$

We introduce a new dimensionless parameter (ϕ) at this point of derivation and the final modified form of the vapor phase model can be given by Equation 8 in Table 3.

Table 3: Vapor phase steady-state BCR model for methanol and water

Species (Vapor)	Steady state CBCR vapor model
i = Methanol or Water	$p_i^V = \frac{p_{i_0}^V + \phi H_i C_i^L}{1+\phi}$ [8]

where, $\phi = \frac{(ka)}{(\dot{v}_{V_0}/V_L)}$ [9]

Equation 8 gives the steady state vapor phase model and acts as an explicit expression for methanol (or water) partial pressure in the vapor phase. It is advantageous to replace the methanol or water partial pressure terms during the liquid phase modeling. The newly introduced parameter 'ϕ' can be used in determining the impacts of the limiting behavior of the alcohol feed rate into the system which can be defined as the ratio of gas residence time to characteristic time for absorption into oil.

Liquid Phase Modeling: The liquid phase transient mass balances are given by,

i = MeOH/Water (liquid):
$$\frac{d\left(V_L C_i^L\right)}{dt} = \dot{v}_{L_0}\left(C_{i_0}^L - C_i^L\right) + r_i V_L - \dot{n}_{i,mt} \quad [10a]$$

j = FFA/FAME (liquid):
$$\frac{d\left(V_L C_j^L\right)}{dt} = \dot{v}_{L_0}\left(C_{j_0}^L - C_j^L\right) + r_j V_L \quad [10b]$$

Where, $C_{i\,or\,j}^L$ are the liquid phase concentrations of methanol, water, FFA or FAME respectively. $\dot{v}_{L_0}$ is the liquid flow rate which is constant for both feed and outlet streams, V_L is the liquid volume.

Substituting for the rate law and interphase mass transfer expressions from equation 1 and 2 into above set of differential balances, we get

Methanol (liquid): $$\frac{d(V_L C_M^L)}{dt} = \dot{v}_{L_0}(C_{M_0}^L - C_M^L) - V_L(k_f C_F^L C_M^L - k_r C_B^L C_W^L) - (ka)V_L(C_M^{V^*} - C_M^V) \quad [11a]$$

Water (liquid): $$\frac{d(V_L C_W^L)}{dt} = \dot{v}_{L_0}(C_{W_0}^L - C_W^L) + V_L(k_f C_F^L C_M^L - k_r C_B^L C_W^L) - (ka)V_L(C_W^{V^*} - C_W^V) \quad [11b]$$

FFA (liquid): $$\frac{d(V_L C_F^L)}{dt} = \dot{v}_{L_0}(C_{F_0}^L - C_F^L) - V_L(k_f C_F^L C_M^L - k_r C_B^L C_W^L) \quad [11c]$$

FAME (liquid): $$\frac{d(V_L C_B^L)}{dt} = \dot{v}_{L_0}(C_{B_0}^L - C_B^L) + V_L(k_f C_F^L C_M^L - k_r C_B^L C_W^L) \quad [11d]$$

The oil phase is dilute in methanol and water. Also, because the FFA and FAME densities are approximately the same, we assume that the total concentration of the liquid phase is constant and can be given by the sum of the free fatty acid and biodiesel concentrations. This can be mathematically expressed as:

$$C_L = C_B^L + C_F^L \xrightarrow{\text{differentiating}} \frac{dC_F^L}{dt} = -\frac{dC_B^L}{dt} \quad [12]$$

This reduces the set of differential equations to three couple non-linear equations instead of four. Defining $\tau_L = \frac{V_L}{\dot{v}_{L_0}}$ as the liquid residence time in hours/time scale and $K_{eq} = \frac{k_f}{k_r}$ as the reaction equilibrium constant, and substituting for vapor phase concentrations using ideal gas law and then Henry's law, the new liquid phase model is:

Methanol (liquid): $$\frac{dC_M^L}{dt} = \frac{(C_{M_0}^L - C_M^L)}{\tau_L} - k_f\left(C_F^L C_M^L - \frac{C_B^L C_W^L}{K_{eq}}\right) - \frac{(ka)}{RT}(H_M C_M^L - p_M^V) \quad [13a]$$

Water (liquid): $$\frac{dC_W^L}{dt} = \frac{(C_{W_0}^L - C_W^L)}{\tau_L} + k_f\left(C_F^L C_M^L - \frac{C_B^L C_W^L}{K_{eq}}\right) - \frac{(ka)}{RT}(H_W C_W^L - p_W^V) \quad [13b]$$

FFA (liquid): $$\frac{dC_F^L}{dt} = -\frac{dC_B^L}{dt}$$ [13c]

FAME (liquid): $$\frac{dC_B^L}{dt} = \frac{\left(C_{B_0}^L - C_B^L\right)}{\tau_L} + k_f\left(C_F^L C_M^L - \frac{C_B^L C_W^L}{K_{eq}}\right)$$ [13d]

Using vapor-phase model (equation 8) we can substitute for the partial pressures of methanol and water in the above differential balances which will eliminate the dependence on real-time species partial pressure and reduce the equations in terms of vapor pressure in feed and liquid phase concentrations of methanol and water. Hence, using vapor phase model (equation 8) into the above set and further algebraic simplification, the final modified form of the raw liquid phase transient model can be given by a set of four coupled non-linear ODEs presented in Table 4 (equations 14a-14d).

Table 4: Liquid phase dynamic bubble column reactor model

Species (Liquid)	**Dynamic CBCR liquid model**	
Methanol	$\frac{dC_M^L}{dt} = \frac{\left(C_{M_0}^L - C_M^L\right)}{\tau_L} - k_f\left(C_F^L C_M^L - \frac{C_B^L C_W^L}{K_{eq}}\right) - \frac{(ka)}{RT(1+\phi)}\left(H_M C_M^L - p_{M_0}^V\right)$	[14a]
Water	$\frac{dC_W^L}{dt} = \frac{\left(C_{W_0}^L - C_W^L\right)}{\tau_L} + k_f\left(C_F^L C_M^L - \frac{C_B^L C_W^L}{K_{eq}}\right) - \frac{(ka)}{RT(1+\phi)}\left(H_W C_W^L - p_{W_0}^V\right)$	[14b]
FAME	$\frac{dC_B^L}{dt} = \frac{\left(C_{B_0}^L - C_B^L\right)}{\tau_L} + k_f\left(C_F^L C_M^L - \frac{C_B^L C_W^L}{K_{eq}}\right)$	[14c]
FFA	$\frac{dC_F^L}{dt} = -\frac{dC_B^L}{dt}$	[14d]

3.2.6. Nondimensionalization of Reactor Model

The model was further simplified be redefining the state variables in dimensionless form to reduce the number of model parameters. The concentrations and the partial pressures were non-dimensionalized according to the following definitions,

$$\xi = \frac{C_B^L}{C_L} \quad [15a] \qquad \xi' = (1-\xi) = \frac{C_F^L}{C_L} \quad [15d]$$

$$\alpha_M = \frac{C_M^L}{\left({}^{P_{atm}}/_{H_M}\right)} \quad [15b] \qquad \alpha_W = \frac{C_W^L}{\left({}^{P_{atm}}/_{H_W}\right)} \quad [15e]$$

$$y_{M_0} = \frac{p_{M_0}^V}{P_{atm}} \quad [15c] \qquad y_{W_0} = \frac{p_{W_0}^V}{P_{atm}} \quad [15f]$$

Where, ξ, α_M, α_W are the new dimensionless state variables and y_{M_0}, y_{W_0} are known dimensionless input process variables. Upon introducing the above definitions into the final raw model and further algebraic manipulation, we arrive at the following set of equations given by,

$$\frac{d\alpha_M}{dt} = \frac{(\alpha_{M_0} - \alpha_M)}{\tau_L} - k_f C_L \left((1-\xi)\alpha_M - \frac{\xi \alpha_W H_M}{K_{eq} H_W}\right) - \frac{(ka)H_M}{RT(1+\phi)}(\alpha_M - y_{M_0}) \quad [16a]$$

$$\frac{d\alpha_W}{dt} = \frac{(\alpha_{W_0} - \alpha_W)}{\tau_L} + k_f C_L \left(\frac{H_W}{H_M}\right)\left((1-\xi)\alpha_M - \frac{\xi \alpha_W H_M}{K_{eq} H_W}\right) - \frac{(ka)H_W}{RT(1+\phi)}(\alpha_W - y_{W_0}) \quad [16b]$$

$$\frac{d\xi}{dt} = \frac{(\xi_0 - \xi)}{\tau_L} + \frac{k_f P_{atm}}{H_M}\left((1-\xi)\alpha_M - \frac{\xi \alpha_W H_M}{K_{eq} H_W}\right) \quad [16c]$$

$$\frac{d\xi'}{dt} = -\frac{d\xi}{dt} \quad [16d]$$

At this point of the derivation, two new characteristic time scales (τ_R and τ_A) and two new dimensionless parameters (β and θ) were defined to simplify the model,

$$\beta = \frac{H_W}{H_M} \quad [17a] \qquad \theta = \frac{C_L H_M}{P_{atm}} \quad [17b]$$

$$\tau_R = \left(\frac{1}{k_f}\right)\left(\frac{H_M}{P_{atm}}\right) \quad [17c] \qquad \tau_A = \frac{RT(1+\phi)}{H_M(ka)} \quad [17d]$$

Substituting the above definitions into the model we arrive at the complete simplified transient model of the liquid phase which is given by the set of four non-linear couple differential equations presented in Table 5.

Table 5: Reduced form of liquid phase dynamic bubble column reactor model

Species (Liquid)	**Reduced dynamic CBCR liquid model**	
Methanol	$\frac{d\alpha_M}{dt} = \frac{(\alpha_{M_0} - \alpha_M)}{\tau_L} - \frac{\theta}{\tau_R}\left(\alpha_M(1-\xi) - \frac{\alpha_W \xi}{K_{eq}\beta}\right) - \frac{1}{\tau_A}(\alpha_M - y_{M_0})$	[18a]
Water	$\frac{d\alpha_W}{dt} = \frac{(\alpha_{W_0} - \alpha_W)}{\tau_L} + \beta\frac{\theta}{\tau_R}\left(\alpha_M(1-\xi) - \frac{\alpha_W \xi}{K_{eq}\beta}\right) - \beta\frac{1}{\tau_A}(\alpha_W - y_{W_0})$	[18b]
FAME	$\frac{d\xi}{dt} = \frac{(\xi_0 - \xi)}{\tau_L} + \frac{1}{\tau_R}\left(\alpha_M(1-\xi) - \frac{\alpha_W \xi}{K_{eq}\beta}\right)$	[18c]
FFA	$\frac{d\xi'}{dt} = -\frac{d\xi}{dt}$	[18d]

Equations 18a – 18d approximates the behavior of the two phase bubble column reactor used for biodiesel production from high FFA content oils as described in Figure 14. Each term in this model has dimensions of $(\text{time})^{-1}$ which are the characteristic time scales for each type of physical mechanisms described by the model. The explicit appearance of liquid residence time in the model makes it flexible to be used in either continuous or semi-batch modes by setting large or small values of τ_L.

3.3. Description of Model Parameters

There are several parameters in the reduced model which are listed in Table 6 along with their definitions and physical meanings. These parameters characterize the transport mechanics and kinetics of the bubble column reactor. They are adjustable parameters that can be used identify the optimum steady state(s) and the operational regime of the bubble column reactor.

Table 6: List of model parameters and their definitions

Parameter	**Expression**	**Definition**
ϕ	$\frac{(ka)}{\left(\dot{v}_{V_0}/V_L\right)}$	ratio of rate of absorption to rate of vapor gas turnover per volume of liquid
τ_R	$\left(\frac{1}{k_f}\right)\left(\frac{H_M}{P_{atm}}\right)$	characteristic time scale of forward reaction in liquid phase
τ_A	$\frac{RT(1+\phi)}{H_M(ka)}$	characteristic time of methanol absorption into liquid phase
Da	$\frac{\tau_A}{\tau_R} = \frac{k_f P_{atm} RT(1+\phi)}{H_M^2(ka)}$	modulus of $\tau_A$to τ_R produces a Damköhler Number
θ	$\frac{C_L H_M}{P_{atm}}$	ratio of initial molar concentration of FFA to maximum methanol content in oil
β	$\frac{H_W}{H_M}$	ratio of maximum moles of methanol to water in liquid phase

(a) $\boldsymbol{\phi}$ **–** This dimensionless parameter arises from the vapor phase model which affects the maximum amount of methanol dissolved in liquid phase. It contains vapor feed rate in the denominator and it indirectly influences the speed of methanol transport to the oil phase (via interphase mass transfer term) and the maximum amount of methanol available for reaction in the liquid phase. If the vapor feed rate is high, there is a small amount of time available for methanol transport into the oil phase from vapor phase and most of the methanol will be vented off without reacting. This leads to the oil becoming saturated in methanol more rapidly so that $p_i^V = p_{i_0}^V$. Conversely, if the vapor feed rate is low ($\phi \rightarrow \infty$) methanol in vapor phase will be at equilibrium with methanol in liquid phase which will make rate of reaction slower. The operating limits of this parameter can be represented mathematically as:

$$\phi \rightarrow \begin{cases} 0, \text{ for high vapor feed rate} \\ \infty, \text{ for low vapor feed rate} \end{cases} \quad [19]$$

Hence the limiting behavior of the vapor phase model can be approximated as,

$$p_i^V \approx \begin{cases} p_{i_0}^V & \text{as } \phi \rightarrow 0 \\ H_i C_i^L & \text{as } \phi \rightarrow \infty \end{cases} \quad [20]$$

(b) $\boldsymbol{\tau_R}$ **and** $\boldsymbol{\tau_A}$ – These two parameters are the characteristic reaction time and transport time created by dividing the forward reaction rate constant and the mass transfer coefficient with their respective scales. The ratio of both of these scaled variables provides a useful dimensionless parameter called the Damköhler Number (Da) which is the ratio of the velocity of methanol consumption via esterification reaction to the velocity of methanol absorption into the liquid phase. Hence, it is a measure of the intrinsic reaction rate to that of methanol absorption. The Damköhler number has not been incorporated into the dimensionless model explicitly, but it provides an estimate of

the operating regime of the reactor during the simulation. From the expression of the Damköhler Number, we can see that the parameter 'ϕ' appears in the numerator and it can be concluded that the impact of vapor feed rate strategy appears in the model via the Damköhler Number. Damköhler Numbers have been frequently used in biodiesel production processes to study kinetic limited regimes (*79*).

This number indicates that if we are interested in studying diffusion-limited conditions (Da $\rightarrow \infty$) of the bubble column reactor, in this case the diffusion of methanol into liquid phase from vapor phase is very slow compared to reaction (*80*). This means that diffusion is the controlling step and almost all the methanol being absorbed in the liquid phase instantaneously reacts to form biodiesel. This will result in low biodiesel conversion, long conversion times and longer operational hours which is not desirable in a scale up point of view. As for high vapor feed rates ($\phi \rightarrow 0$), the methanol absorption occurs at a low but constant rate which is relatively slower than the speed of the reaction. This leads to lower conversion due to diffusion-limited conditions and less availability of methanol in the liquid phase. Most of the methanol entering the system via vapor feed escapes and the methanol vapor pressure in the reactor remains the same as the inlet feed pressure. This is not a desirable operating strategy under scale up conditions.

On the other hand, if we are interested in studying the kinetics-limited conditions (Da $\rightarrow 0$) of the BCR, then in this case the speed of reaction is very slow compared to the velocity of methanol absorption into the liquid phase (*80*). This means that reaction is the controlling step and there will be methanol build-up in the liquid phase due to relatively slow consumption of methanol by the reaction than the amount diffusing into the liquid phase from vapor side. This will result in high conversion but take long duration to reach

desirable conversion. For low vapor feed rates ($\phi \rightarrow \infty$), methanol absorption occurs relatively faster than the reaction which leads to kinetics-limited conditions where the methanol exists at equilibrium within the system. Due to continuous availability of excess methanol, a high overall conversion is achievable but at the cost of long durations, which is also not a desirable operating strategy for the reactor.

(c) θ and β – These two parameters are dimensionless and are characteristic to the physical properties of the system at a particular temperature and pressure. *'β'* measures the ratio of maximum solubility of methanol to water in the oil phase. *'θ'* is an approximate measure of the maximum saturation of methanol at atmospheric pressure in the vapor phase also defined as the ratio of initial molar concentration of FFA to maximum methanol content in oil.

(d) K_{eq} – The equilibrium constant appears in the reduced model explicitly which is useful in exploring the equilibrium limitations of the system using this parameter.

3.4. Numerical Algorithm and Simulation Procedure:

The bubble column reactor can be approximately described by the four coupled differential equations [Equations 18a – 18d] together with the initial conditions. The initial conditions varied depending on the type of desired studies. For the transient studies, the initial conditions were similar to the feed conditions to the reactor. The reactor is fed with pure FFA while the methanol feed conditions changed according to the study performed in terms of quality and flow rate. For simplicity, first-order Euler's forward finite difference algorithm was employed to numerically integrate the set of differential equations in Excel. The time step (Δt) was chosen to be 0.002h (7.2s) to

ensure conditional stability and bounded solutions. Euler's 1st order forward method is an explicit numerical method used to determine a variable at a future time step based on its known values at present time step. The algorithm is given as:

$$y(t_{i+1}) = y(t_i) + \Delta t * f_y\{t_i, \alpha_M(t_i), \alpha_W(t_i), \xi(t_i)\} \quad [21]$$

Where, 'y' is one of the three state variables of the model (α_M, α_W or ξ) evaluated at i^{th} instant of time and f_y is the function describing the temporal gradient of the state variable 'y'. First order Euler's forward algorithm is associated with a local truncation error (LTE) of the order of $O(\Delta t^2)$. This arises due to the origin of the algorithm from truncated Taylor Series expansion around a neighboring area of $t = t_i$ is given as:

$$y(t_i + \Delta t) = y(t_i) + \Delta t * f_y\{t_i, \alpha_M(t_i), \alpha_W(t_i), \xi(t_i)\} + O(\Delta t^2) \quad [22]$$

3.5. Parameter Estimation & Model Validation

The objective of the parameter estimation was to obtain reliable estimates for the characteristic methanol absorption and forward reaction time scales (τ_A and τ_R), equilibrium constant and theta (θ). Two sets of biodiesel conversion data from semi-batch experiments at pure methanol vapor feed and impure methanol feed with 20 percent v/v water content was considered for the non-linear curve fitting process. A sum of squared errors (SSE) index, the residuals between model predictions and conversion data was calculated and minimized iteratively to estimate the best fit using Excel's iterative 'Solver' function. Generalized Reduced Gradient method was opted explicitly along with imposing non-negative parameter constraint for solving.

In semi-batch operation, the residence time is infinite ($\tau_L \to \infty$). In the model this was approximated by setting a high value of $\tau_L = 1000$ h, but for $\tau_L > 10$h, semi-batch operation can still be observed as it is larger than observed conversion times in the laboratory (approximately 2.5 h). Mass transfer coefficients of both methanol and water were assumed to be same so their ratio was approximated to be unity. Methanol was considered less soluble in oil than water and their ratio of maximum solubility (β) was set to 0.5. An initial guess of the characteristic reaction (τ_R) and mass transfer (τ_A) time scales, theta (θ) and equilibrium constant (K_{eq}) was provided to solve the equations before beginning the non-linear curve fitting.

For *'n'* experimental points, the squared residual objective function can be given as:

$$R^2 = SSE = \sum_{j=1}^{n} \left[\xi(t_j) - \bar{\xi}(t_j, \tau_R, \tau_A, \theta, \beta, K_{eq})\right]^2 \quad [23]$$

where, $\xi(t_j)$ is experimental biodiesel conversion data at time *'j'* from measurement set, $\bar{\xi}(t_j, \tau_R, \tau_A, \theta, \beta, K_{eq})$ is model prediction of biodiesel conversion at time *'j'* from experimental conditions same as the measurement set, '*n*' is the number of measurements available for the biodiesel conversion, and the parameters being estimated are τ_R, τ_A and K_{eq}. This objective function was minimized using 'Solver' function built in Microsoft Excel 2010.

Experimental biodiesel conversion data were obtained for both pure methanol feed and impure methanol feed with 20 percent water by volume. These semi-batch experiments were carried out in a graduated cylinder as a bubble column reactor. The reaction temperature was set at 120°C. 70 mL of oleic acid was heated till the reaction temperature

is achieved. Methanol was fed at 0.33 mL/min and sulfuric acid was used as a catalyst in the amount of 0.7 wt% of oil. As mentioned in the experimental section, conversion data were obtained via titration of collected samples using phenolphthalein as the indicator.

The relationship between the parameters being estimated and the biodiesel conversion measurements can be seen from the final model equations of the liquid phase (Table 5). The measurement of conversion *'ξ'* is directly influenced by the parameters,τ_R, K_{eq} and β due to the biodiesel accumulation equation while it is indirectly influenced by τ_A and θ. During the parameter estimation it is desired to capture the plateauing effect of reaction on methanol concentration in oil phase and increase in FFA conversion with progression of time. Also it is desired to capture the effect of increasing water content in vapor feed on FFA conversion and methanol equilibrium.

3.6. Results & Analyses

3.6.1. Introduction

The model is expected to serve the primary role of being able to capture the effects of mass transfer and kinetic limitations of the process on biodiesel conversion. The model was validated using data from semi-batch experiments to obtain values of some of the model parameters. These parameters were then used to conduct parametric studies and measure the reactor performance for varying vapor feed quality and feed rate.

3.6.2. Parameter Estimation & Model Validation

From the curve fitting process we found that there are three ratios of the characteristic time scales (or three ranges of Damköhler number) which provide acceptable approximations to our current data for pure and impure methanol feed. These ranges refer to high, medium and low Damköhler Numbers which represent the performance regime of the bubble column reactor under given experimental conditions. Figures 15a – 15e display several curve fit comparisons between the model and experimental data at different Damköhler numbers. The highest Damköhler number (Da = 4.8) set of parameters produced the least SSE and best fit the data from pure methanol feed study (refer to Table 7), which indicates that the model is able to predict conversions when pure methanol is fed and the reactor is operating under mass transfer limited conditions. In this limit (high Da) reaction is faster than mass transfer as soon as methanol is absorbed into the liquid phase, it is consumed due to reaction and conversion is achieved.

Table 7: List of parameters and values obtained during regression analysis of dynamic model with semi-batch experiments

Study	K_{eq}	τ_A	τ_R	θ	Da	**SSE (Pure Methanol)**	**SSE (80% Impure Methanol)**
1	15	0.07	0.12	6	0.6	0.0412	0.0690
2	30	0.07	0.12	6	0.6	0.0415	0.0599
3	40	0.01	0.35	6	0.03	0.0175	0.0292
4	15	0.01	0.35	6	0.03	0.0176	0.0439
5	1.7	0.048	0.01	6	4.8	0.0098	0.2012

In order to discriminate the validated model, we expanded our fitting procedure to include another set of data where water content of the methanol supply was varied. We used the data from the experiment conducted with 20 percent water content by volume in the methanol feed to determine the ability of the model to capture reactor performance under equilibrium limitations. In this case we found that the model with the highest Damköhler number (study 5 and Figure 15e) set of parameters was unable to capture the impure methanol feed data set producing the highest SSE of the set (SSE = 0.2). Upon inspection, we found that estimation of the equilibrium constant had a significant impact on predicting the dilute vapor feed results. In medium Damköhler number range (Da = 0.6) varying the equilibrium constant from 15 to 30, improved 20% water study SSE by 14% (from 0.069 to 0.059). For low Damköhler number range (Da = 0.03) varying the equilibrium constant from 15 to 40 improved the 20% water study by 33.5% (from 0.00439 to 0.0292). Using the equilibrium constant as an adjustable parameter we found that higher K_{eq} produced lower error and study 3 produced the least SSE when compared to the data from experiment conducted with 20 percent water by volume in the methanol vapor feed. Using this parameter set, the model was able to capture the slower conversion quantitatively due to equilibrium limitations of the reaction when water is present in vapor feed (Figure 15c). We found that the value of the equilibrium constant affected the quality of fit for the impure methanol feed but had negligible influence for the pure methanol feed data. We concluded that the set of data producing the best fit for both pure and impure methanol studies is study 3 $\left(K_{eq} = 40, \tau_A = 0.01,\ \tau_R = 0.35, \theta = 6, \beta = 1\right)$. This set of parameters produces model robust enough to capture the effects of varying vapor feed conditions and the mass transfer dynamics on the final conversion.

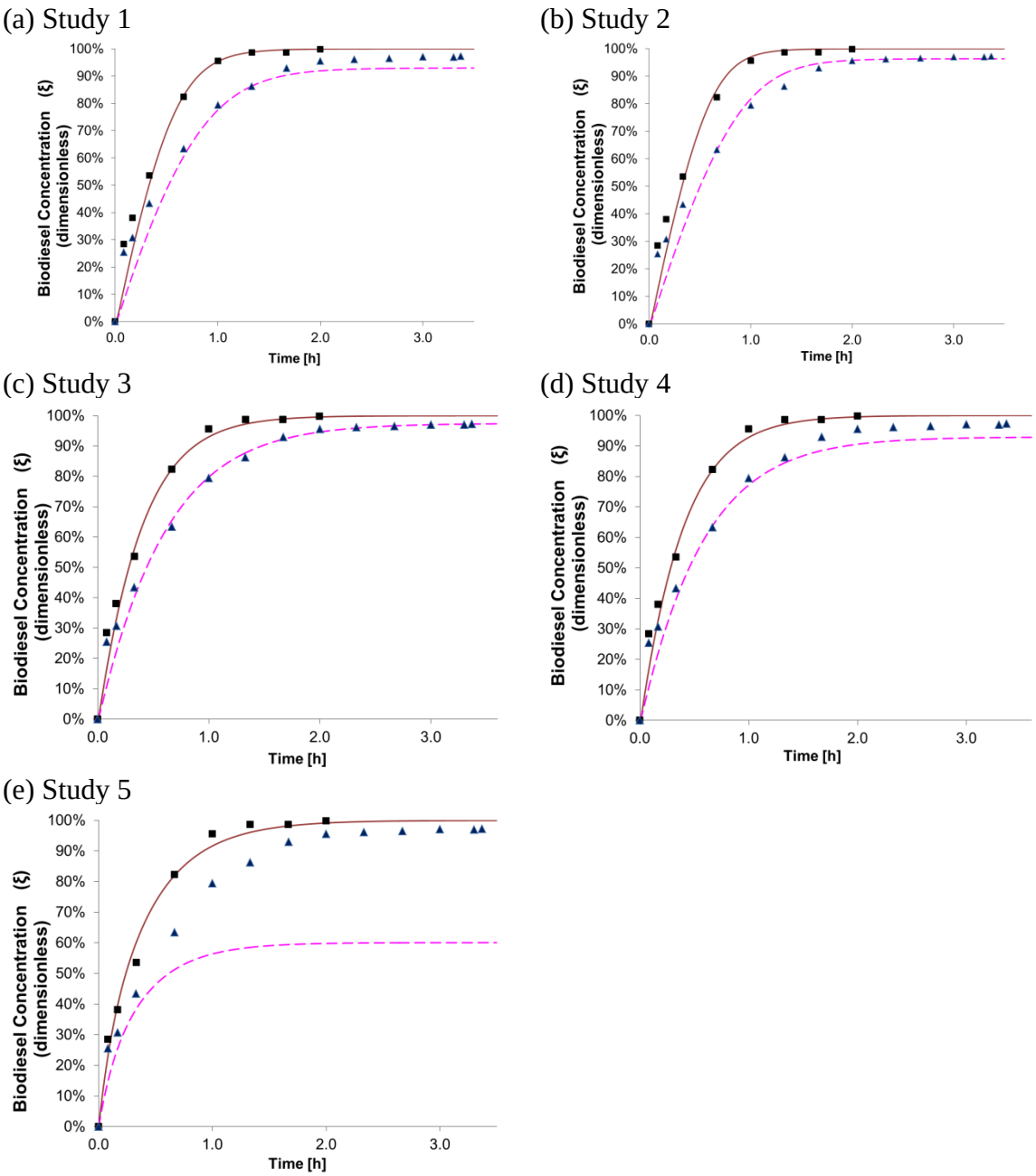

Figure 15: Quality of fit for parameter estimation based on experimental measurements of biodiesel conversion. Solid lines and dashed lines represent model predictions at 0% and 20% water content in vapor feed respectively. Squared markers and triangle markers represent experimental data from semi-batch experiments at 0% and 20% water content in vapor feed respectively.

3.6.3. Typical Predictions of Semi-Batch Model

Figure 16 shows model predictions for the concentrations profile of FFA, FAME, methanol and water under pure methanol vapor feed conditions using parameters from study 3 in Table 7. The experimental conversion data from the semi-batch experiment at 120°C and pure methanol feed at 0.33 mL/min has been plotted to show that the model correctly predicts the experimental trend. Conversion starts to plateau at 90 minutes as the free fatty acid concentration in the liquid phase decreases exponentially. The methanol content rises quickly in the liquid phase which indicates that the reactor is operating in a reaction limited regime and that mass transfer resistance is negligible under the specific experimental conditions. The model predictions show that the water content builds up initially very quickly but later decreases in the liquid phase as the reaction progresses. This indicates that as the methanol concentration rises rapidly initially in the liquid phase, reaction occurs fast enough to cause an initial build-up of water. Later as the reaction slows down due to methanol saturation, the water concentration falls slowly to negligible amounts. This also suggests that presence of water in the liquid phase from reaction does not make the process equilibrium limited and the current reaction temperature is effective in removing the residual water from reaction as a vapor. We will later discuss the impacts of equilibrium limitations on conversion due to presence of water in vapor feed.

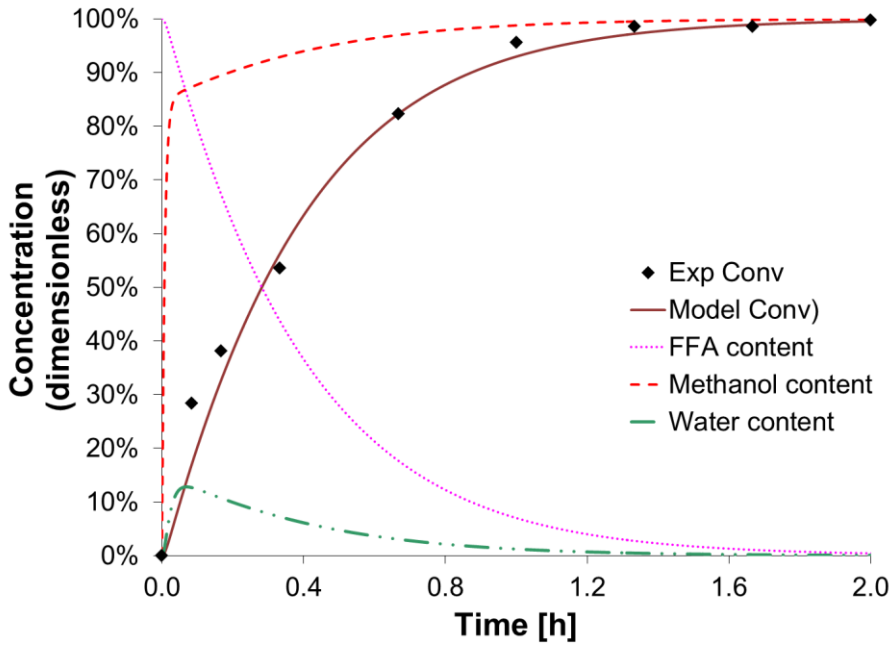

Figure 16: Typical model predictions of concentration profiles of FFA, FAME, methanol and water in liquid phase compared with semi-batch experimental data for pure methanol feed (0% water content) at 120°C and 1 atm.

3.6.4. Robustness Study – Effect of Methanol Vapor Feed Quality

Using the above estimates of the time scales and equilibrium constant representing low Damköhler Number, we examined the model for reasonable representation of experimental data for a wider range of water content in the methanol vapor feed. The model predictions of conversion against data from semi-batch experiments for varying water content in the methanol feed is presented in Figure 17. The model provides a good approximation of the overall conversion data except the first 0.2 h of all the studies. Under this time range all the data set lie at the upper left side of the model predictions. Further explanation of this mismatch is under investigation.

From Figure 18 we can see that the speed of reaction gets slower and and from Figure 17 we see that conversion is achieved at a slower pace as the water content in the

methanol feed increases. The conversion starts plateauing approximately at 90 minutes for pure methanol feed while it occurs at approximately 135 minutes for impure feed. The desired overall conversion (99% - 97%) is not significantly affected from decreasing the methanol feed quality and the model correctly predicts this robust nature of the bubble column reactor towards impure quality of methanol feed. This indicates that the reactor has the potential to operate with feed stream containing recycled methanol and an energy intensive distillation of the methanol exit stream will not be required. This prevents the overall process from high operating and capital cost, thus improving the economic feasibility of the process.

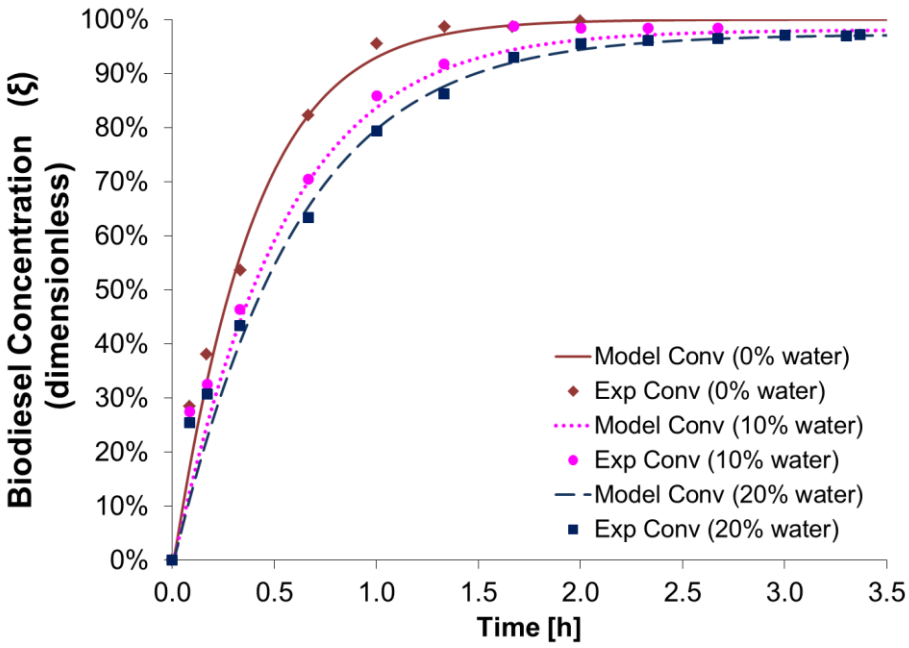

Figure 17: Model predictions of conversion profiles compared with semi-batch experimental data showing impact of varying water content as an impurity in methanol feed on biodiesel yield

3.6.5. Effect of Reaction

In this study, mass transfer of methanol and its availability in the oil phase has a high impact on conversion. Under the given reaction conditions (120°C, 1atm) it is a possibility that most of the methanol might simply vaporize because of its high vapor pressure (*62*). Methanol concentration is a crucial parameter in controlling the reaction rate. Thus the methanol saturation in liquid phase was studied for different vapor feed qualities and methanol feed rates.

From our model we can see that methanol supply rate and its quality plays a significant role in determining the speed of methanol flux into the liquid phase. The model was used to predict methanol availability limit and reaction rate in the liquid phase as it directly influences our understanding of the observed conversion and the model predictions. Figure 18 shows the methanol concentration profile as the reaction progresses. We can see that methanol transports into the liquid phase and saturates faster in the absence of reaction. The level of saturation depends on the purity of the methanol feed as it tends to saturate at the molar percent it was fed into the reactor in the vapor feed. In Figure 18 methanol saturates at 100% and 64% molar percent in the liquid phase for vapor feeds containing 0% and 20% water by volume. In the presence of the reaction we see that the methanol achieves saturation in the liquid phase slower which indicates that the mass transport competes with the consumption of methanol due to reaction. There is always an offset between the no reaction curve and the reaction curve of methanol concentration in the liquid phase clearly indicating the model is able to successfully predict the effect of reaction on the methanol availability in the oil phase. The reaction rate curve rises rapidly initially for a very short amount of time as methanol

concentration increases in the liquid phase but reverses its trend as methanol content starts to saturate in the oil. This decreases the driving force for molar influx of methanol into liquid phase and reaction rate falls due to which conversion starts to plateau.

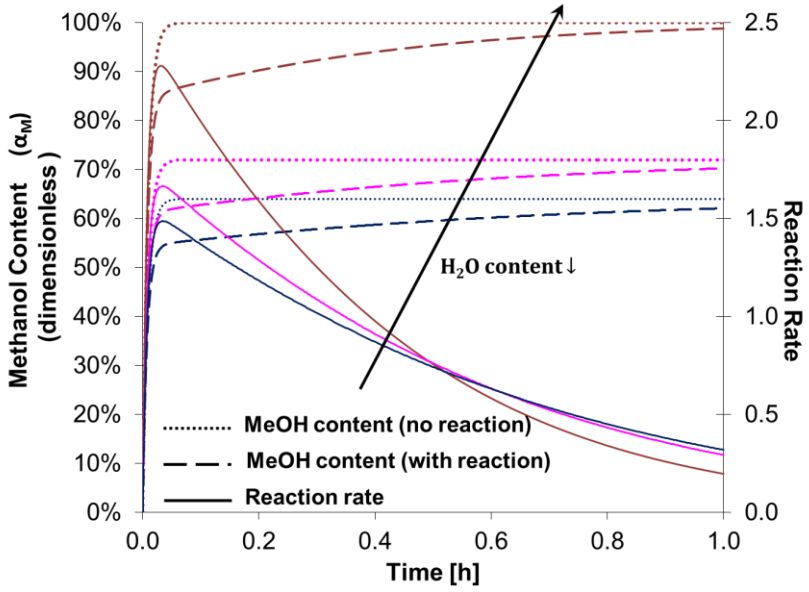

Figure 18: Primary y-axis shows model predictions of methanol saturation profile in the presence (dashed lines) and absence (dotted lines) of reaction for different levels of methanol feed purity (0%, 10% and 20% respectively). Secondary axis shows model predictions for rate of reaction (continuous lines) along the reaction profile for three different levels of methanol feed purity (0%, 10% and 20% respectively).

3.6.6. Parametric Study of Characteristic Absorption Time Scale

The characteristic absorption time scale appears explicitly in the semi-batch dynamic model lumped with the mass transfer term. It is directly related to the state variables: methanol and water concentrations in liquid phase. The validated semi-batch model was used to perform a parametric sensitivity study of the effects of characteristic absorption time scale on the performance of the bubble column reactor. $\boldsymbol{\tau_A}$ was varied by order of magnitude which produced three different ranges of Damköhler number – low, medium and high and they are listed in Table 8. The Damköhler number was found to have a

significant effect in determining the final conversion and the rate of reaction. Figure 19(a) – 19(h) reports the impact of decreasing absorption time (or decreasing Damköhler number) on conversion, methanol content, reaction rate and water content for two different vapor feed streams containing 0% and 20% water as impurity. The reactor performance in the three regimes were explored and analyzed.

Table 8: List of values for characteristic absorption time scales and Damköhler Number indicating three different operating regimes used in parametric sensitivity study of the dynamic CBCR model

Regime	$\boldsymbol{\tau_A}$**(h)**	$\boldsymbol{\tau_R}$**(h)**	$\boldsymbol{Da}$
Low	0.01	0.3503	0.03
	0.03	0.3503	0.09
Medium	0.11	0.3503	0.31
	0.31	0.3503	0.89
High	1.01	0.3503	2.88
	3.01	0.3503	8.59

It was observed that for low absorption time (Da < 0.1) or fast diffusion of methanol, the conversion in the reactor is kinetics limited. Under this regime, $\boldsymbol{\tau_A}$ has negligible effect on further improving conversion if $\boldsymbol{\tau_A}$ is decreased, because in this regime rate of consumption of methanol by reaction is the controlling mechanism. In other words, methanol is quickly absorbed in the oil and available for reaction with FFA. For high absorption time (Da > 2) or slow diffusion of methanol, the conversion becomes mass transfer limited. In this regime, the conversion profile is straight line which indicates very slow progress of reaction due to unavailability of methanol for reaction and diffusion is the controlling mechanism for the overall conversion achieved in due course of time.

When Damköhler number is in the medium range (0.1 < Da < 2), we can see that there is a shift in operating regime inside the reactor, from kinetics limited regime to a

competitive regime into a diffusion limited regime. The effect of this shift can be seen from the change in concentration profiles of methanol. From Figures 19(c) and 19(d) we can see that there is a shoulder in the methanol concentration profile which represents the shift in operating regime. Initially the methanol concentration rises in the liquid quickly for a as the consumption of methanol is slow due to slow kinetics. As soon as the kinetics picks up in the liquid phase, there is a steady increase in methanol concentration which indicates that the mass transfer is competing with the rate of consumption of methanol. As most of the free fatty acid has been consumed and conversion starts to plateau we can see that the regime shifts to diffusion limited where most of the conversion achieved is controlled by the amount of methanol absorbed in the liquid phase.

Thus from this parametric sensitivity study we can conclude that the semi-batch model is able to successfully capture the impacts of varying operating regimes on overall biodiesel conversion and reactor performance. Detailed examination of the results show that both diffusion limited and kinetics limited behavior can occur in the reactor and they can also coexist.

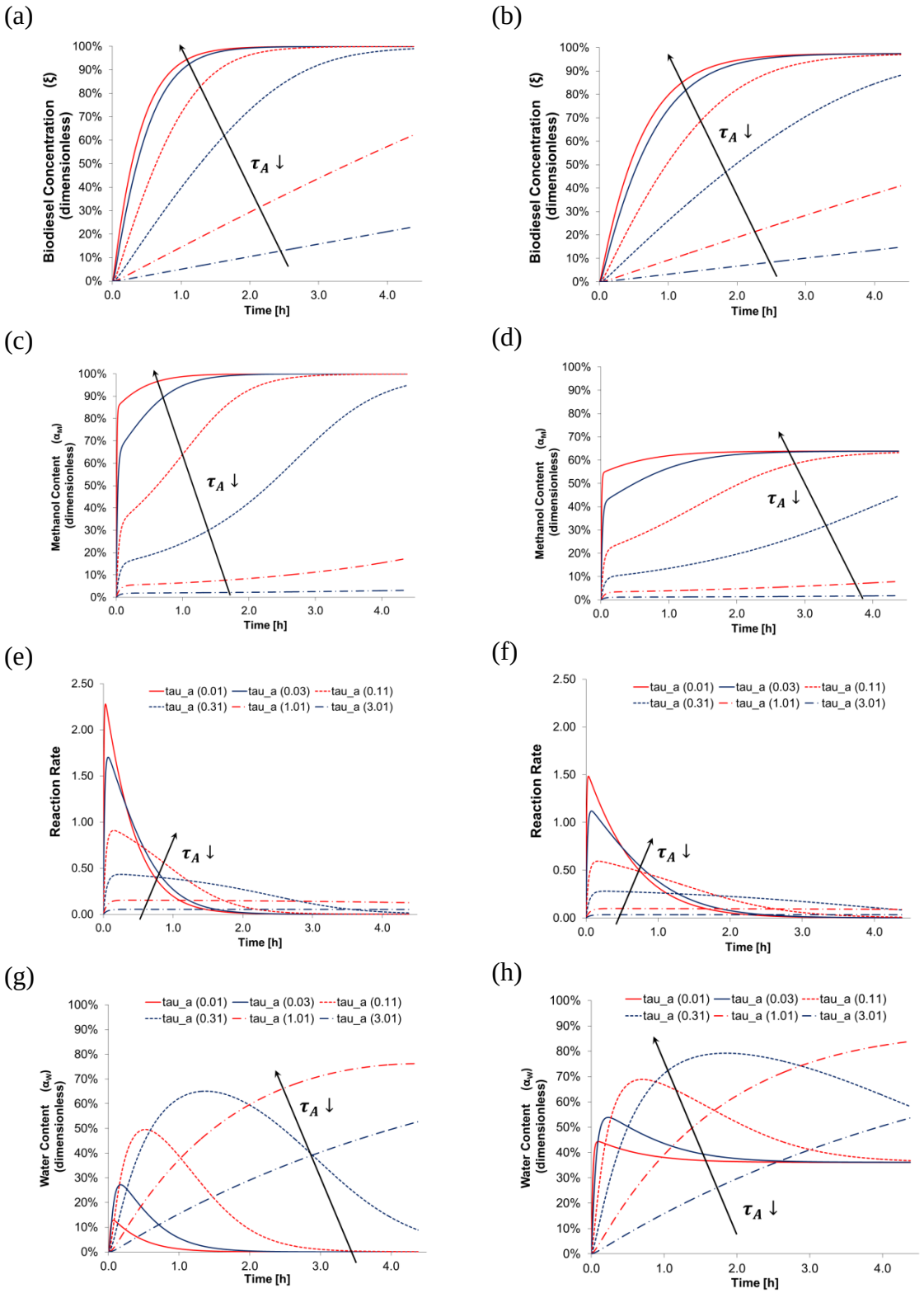

Figure 19: Model predictions of concentration profiles and reaction rates from parametric sensitivity study by varying absorption time scale ($\boldsymbol{\tau_A}$) for both pure methanol (a, c, e, g) and 80% impure methanol (b, d, f, h) feed conditions. $\boldsymbol{\tau_A}$ was varied in three different ranges of magnitude: (0.01h and 0.03h), (0.11h and 0.31h) and (1.01h and 3.01h)

3.6.7. Effect of Methanol Supply Rate

Model predictions were optimized and compared with experimental data from a different set of semi-batch experiments using three different methanol vapor feed rates which can be categorized into low (approximately 0.7mL/h and 0.9mL/h) and high (approximately 1.2mL/h) flow regions. The model parameters used for this study are the same as listed for Study 3 in Table 7 except the characteristic time scale. τ_A was subjected to variation in Excel to produce the least SSE computed according to equation 23. We can see from Figure 20a that the model relatively fits the experimental data for low flow rates until approximately 0.7 hours but later fails to capture the long time conversion data. And the model underestimates the conversion from high methanol flow rates for the entire course of reaction. This mismatch may be because of different experimental conditions (such as higher catalyst concentration) used for the methanol flow rate semi-batch experiments. Figure 20b shows that the methanol concentration (dashed lines) rises rapidly in liquid phase but takes approximately the entire conversion time (~1.2 h) to reach saturation. This is due to the consumption by reaction (continuous lines) as the reaction rate falls along the reaction co-ordinate. Water concentration rapidly rises initially at the beginning of the reaction, but later it lowers and saturates in oil phase as the reaction progresses. This shows that water is able to exit the oil phase without retarding the forward reaction rate.

(a)

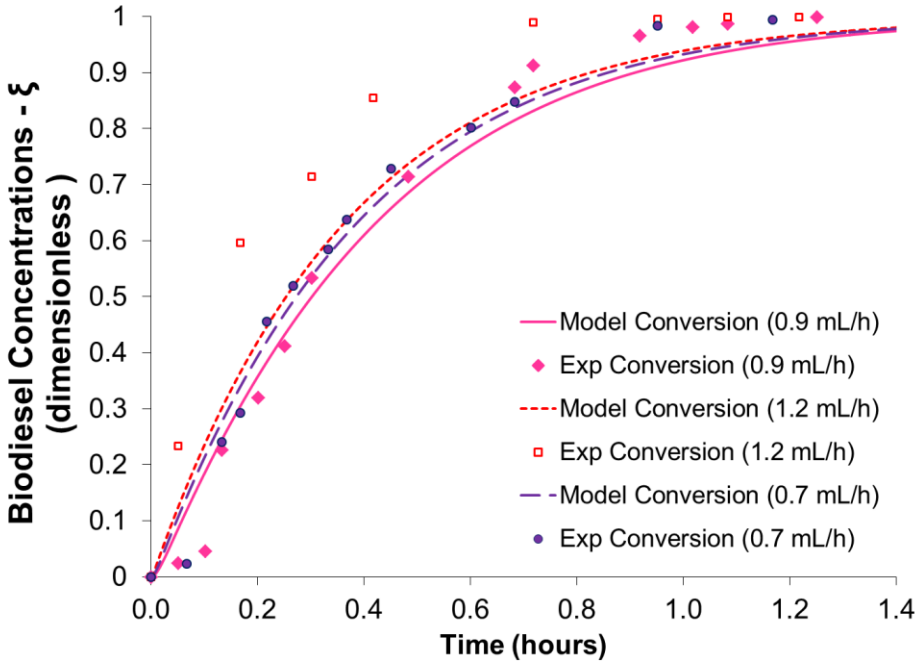

(b)

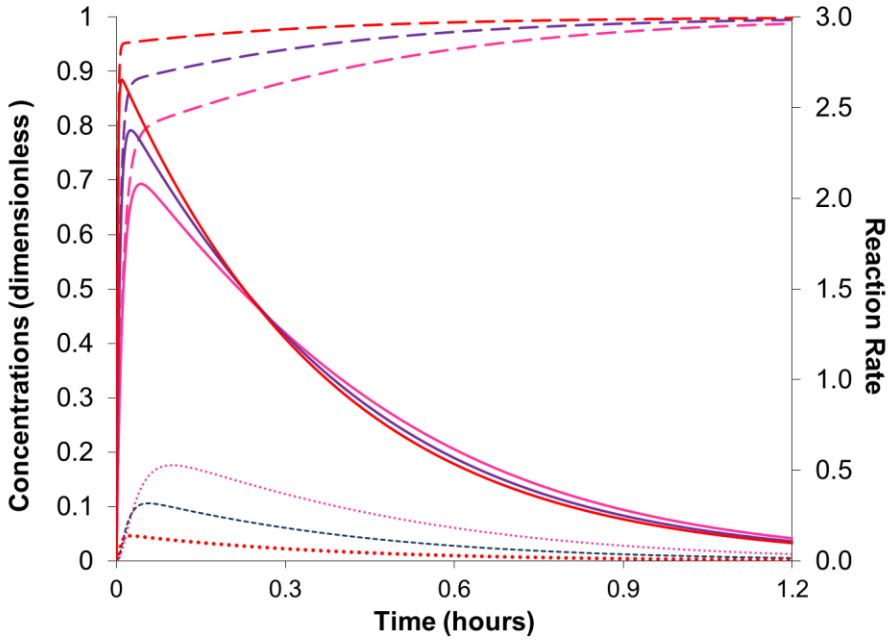

Figure 20: (a) Model predictions and experimental biodiesel conversion profile for two different low (0.9 and 0.7 mL/h) and high (1.7 mL/h) vapor feed rates. Lines represent model predictions while markers represent experimental data. (b) On the primary axis model predictions for concentration profiles of methanol and water has been plotted while on secondary axis reaction rate is plotted. Continuous lines represent reaction rate, dashed and dotted lines represent methanol and water saturation respectively.

4. Bubble Column CSTR Steady State Model

4.1. Introduction

Continuous bubble column reactors can be used for biodiesel production under steady state mode which requires studying the performance of the reactor and establish its optimum scale-up design and operating conditions. From preliminary lab studies conducted by an MEM senior design team, it was found that adding internals inside the reactor improves conversion time compared to reactor without internals. Adding baffles inside the reactor divided the reactor into several zones which gives rise to an approximate plug flow behavior in each section. Each stage could act as an ideal continuously stirred reactor with enhanced residence time. Creating a multistage reactor can provide better performance and prove cost effective depending on the number of stages and cumulative residence time (*70*).

4.2. Description of Bubble Column CSTR Steady State Model

4.2.1. Single Stage Bubble Column CSTR

The transient continuous bubble column CSTR model (Equations 24a – 24d) was transformed into steady state form to perform steady state calculations by setting all of the temporal derivatives equal to zero. This produces a set of non-linear algebraic equations relating the product compositions to feed compositions and operating parameters. The parameters and feed conditions are listed in Table 10 based on the curve fitting results of the dynamic model in Chapter 3. Operating a CSTR in a continuous

mode leads to dilution of the products so that conversion decreases as characteristic residence time decreases. An advantage of this steady state model in comparison to other CSTR models is that it takes into account the mass transfer limitations involved in a gas-liquid bubble column, reversible reaction kinetics and the equilibrium limitations of the system.

4.2.2. Multi Stage Bubble Column CSTR

The single stage steady state model was extended to create a continuous multistage column model with stages connected in series (Figure 21). The set of non-linear algebraic equations 24a -24d in Table 9 represent the steady state design equation for stage *'i'* of the multistage reactor.

Table 9: Design equations for multistage steady state continuous bubble column reactor

Species (Liquid)	**Steady state BCR model**	
Methanol	$\frac{(\alpha_{M_{i-1}} - \alpha_{M_i})}{\tau_L} - \frac{\theta}{\tau_R}\left(\alpha_{M_i}(1-\xi_i) - \frac{\alpha_{W_i}\xi_i}{K_{eq}\beta}\right) - \frac{1}{\tau_A}(\alpha_{M_i} - y_{M_0}) = 0$	[24a]
Water	$\frac{(\alpha_{W_{i-1}} - \alpha_{W_i})}{\tau_L} + \beta\frac{\theta}{\tau_R}\left(\alpha_{M_i}(1-\xi_i) - \frac{\alpha_{W_i}\xi_i}{K_{eq}\beta}\right) - \beta\frac{1}{\tau_A}(\alpha_{W_i} - y_{W_0}) = 0$	[24b]
FAME	$\frac{(\xi_{i-1} - \xi_i)}{\tau_L} + \frac{1}{\tau_R}\left(\alpha_{M_i}(1-\xi_i) - \frac{\alpha_{W_i}\xi_i}{K_{eq}\beta}\right) = 0$	[24c]
FFA	$\xi'_i = 1 - \xi_i$	[24d]

The above equations can approximately describe a cross flow multistage reactor which could be constructed using a horizontal reactor using baffles. A schematic of the cross-flow multistage reactor is illustrated in Figure 21. A cross flow pattern of gas – liquid

streams is assumed such that fresh methanol is added to each CSTR stage. Fresh oil is fed to the first stage and product is removed from the final stage. Methanol vapor feed is fed to each of the stages and comes in contact with oil in a perpendicular direction to the flow of oil across the stages in series. The major assumptions made here is that each stage is of equal volume, has an equal residence time and is completely mixed. In this model there is no backflow mixing between stages. Figure 22 shows the different reactor configurations based on a cross-flow pattern of gas-liquid streams.

The objective of the multistage CSTR model is to study the reactor performance under dilution, the impact of residence time distribution on final overall biodiesel conversion and the effect of "staging" by compartmentalizing the total reactor volume in series. CSTRs connected in series can provide a performance approximated by batch behavior. By varying the number of stages it is also possible to obtain reaction system with performance intermediate of idealized continuous models. This study together with cost information can be used to gain insights about optimizing the number of stages required for achieving the desired biodiesel conversion and design a multistage reactor.

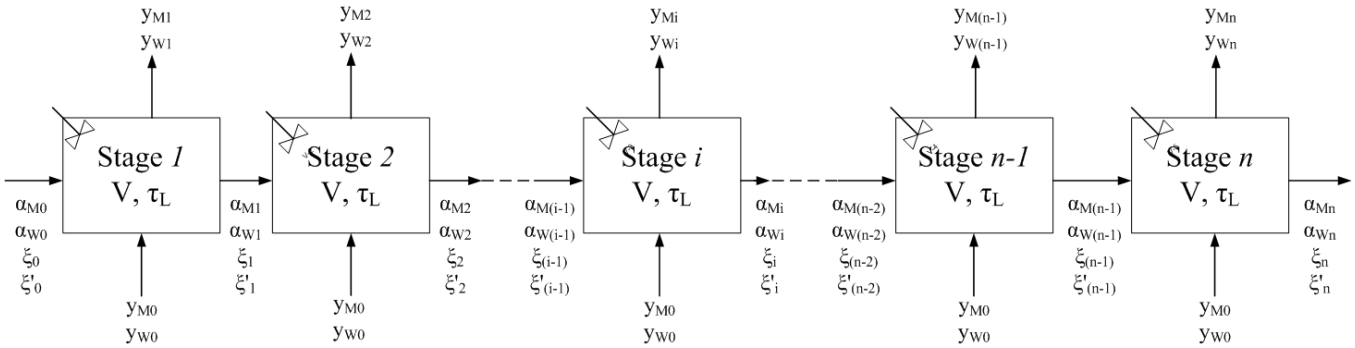

Figure 21: Steady state multistage bubble column reactor model in continuous mode as a cascade of *'n'* CSTRs connected in series incorporating cross flow pattern

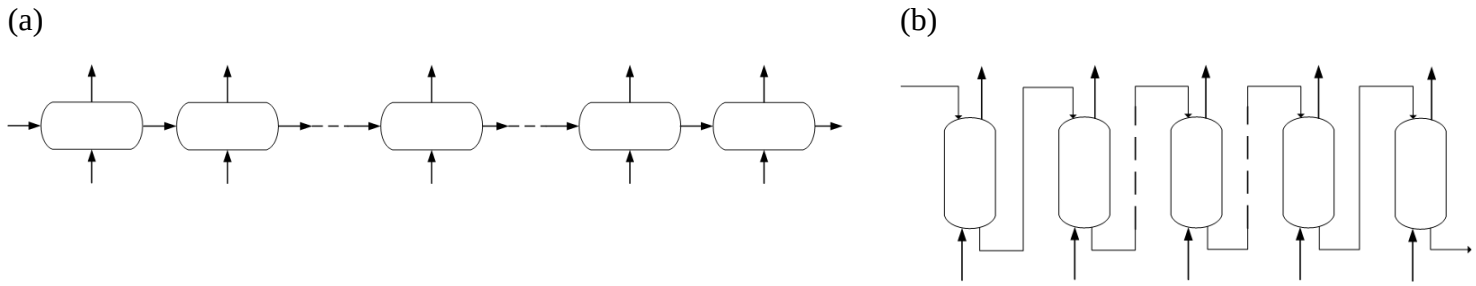

Figure 22: Different configurations of multistage BCRs connected in series exhibiting cross-flow pattern

4.3. Solution Procedure

Using the parameters and the initial conditions listed in Table 10, the steady state multistage model for '*n*' stages was solved as a system of '*4n*' algebraic equations containing *'4n'* unknown variables. The commercial software MAPLE was used to perform the iterative calculations and Excel was used to plot the results. The outlet concentrations of each stage were used as inlet concentrations for all four components in the liquid phase in the model. The vapor inlet concentration for methanol and water was same for every stage as the same vapor feed is distributed into all the stages simultaneously. The outlet liquid phase concentration of methanol (α_M) will vary according to the extent of reaction in each stage and their relative position in the train of stages. This is because the reaction rate will decrease along the train as the amount of free fatty acid decreases and biodiesel increases in the oil phase entering each stage.

Table 10: List of the values of model parameters and reactor inlet conditions used for steady state modeling of bubble column reactor

Parameter	**Value**	**Inlet Conditions**	**Value**
K_{eq}	40	Pure MeOH feed - (y_{M_0}, y_{W_0})	(1,0)
τ_A	0.001	10% water impure MeOH feed - (y_{M_0}, y_{W_0})	(0.72, 0.28)
τ_R	0.3502	20% water impure MeOH feed - (y_{M_0}, y_{W_0})	(0.64, 0.36)
θ	6	Liquid Feed - $(\alpha_{M_0}, \alpha_{W_0}, \xi_0, \xi_0')$	(0, 0, 0,1)
β	0.551		

4.4. Results and Analyses

The multi stage steady state model was solved for different vapor feed quality, different number of stages and different total residence times. The results were also compared with semi-batch model predictions and experimental results to approximate the optimum staging required to achieve a desired biodiesel conversion.

4.4.1. Effect of Residence Time and Staging

The steady state model was solved and the overall biodiesel conversion predictions were plotted as a function of cumulative residence time of the reactor configuration. In Figure 23 the overall conversion profiles predicted by the continuous reactor model for pure methanol vapor feed in different multistage reactor configurations (single, two, four and six stages) has been plotted. From the plots we see that the semi-batch model predictions lie at the highest among all conversion profiles as the semi-batch model approximates an infinite residence time. The overall conversion prediction for the continuous reactor model falls below the semi-batch because fresh oil entering the reactor diluted the products. Steady state conversion increases as the total residence time and number of stages increase. From Figure 23, we can also see that there is an effect of diminishing returns in overall conversion as the number of stages is increased. Figure 24 shows that the model can predict the effect of diminishing returns on total residence time of the reactor as number of stages are increased for achieving a minimum of 90% biodiesel conversion. It should be noted here that total reactor volume is proportional to the cumulative residence time and scales with its trend.

(a)

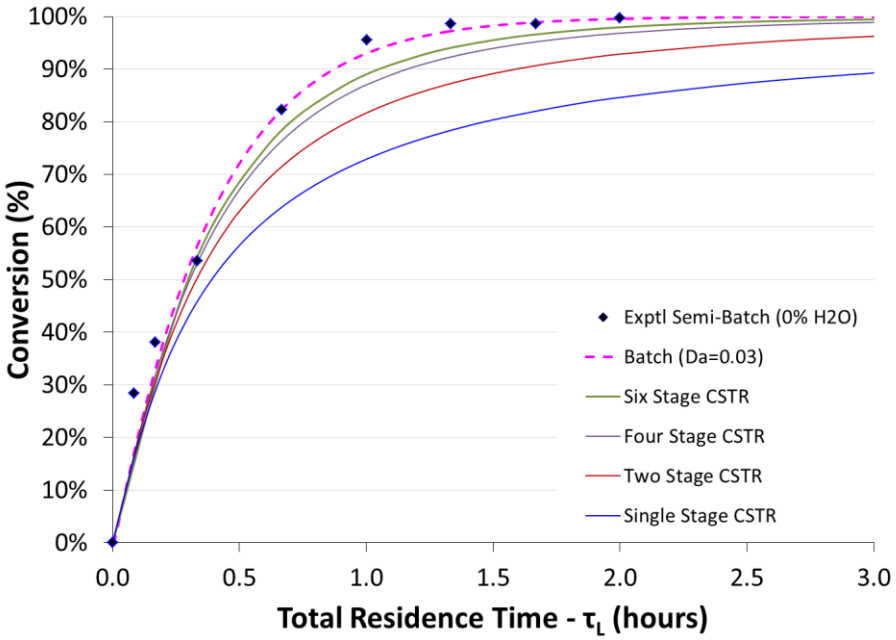

(b)

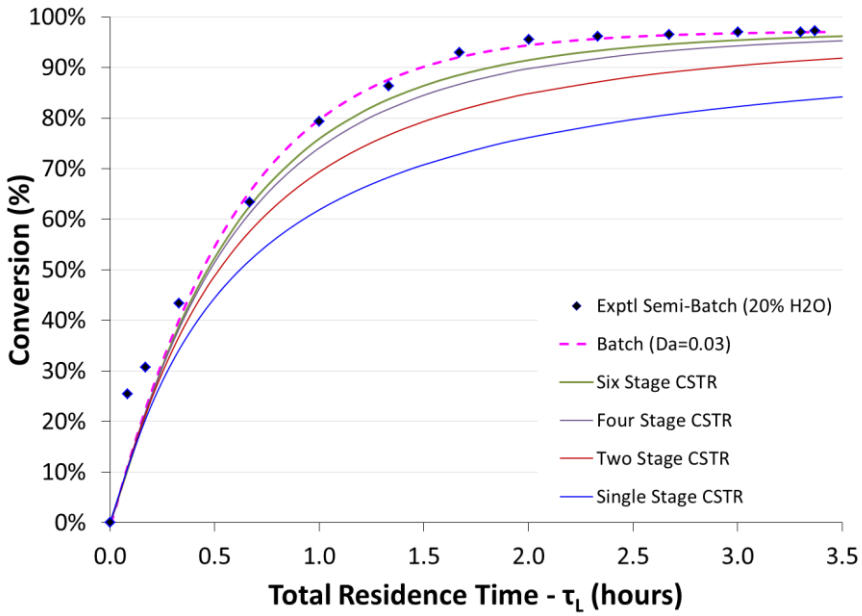

Figure 23: Steady state bubble column reactor model predictions of conversion profiles for different multistage reactor configurations at (a) pure methanol vapor feed, and (b) impure methanol vapor feed with 20% water content

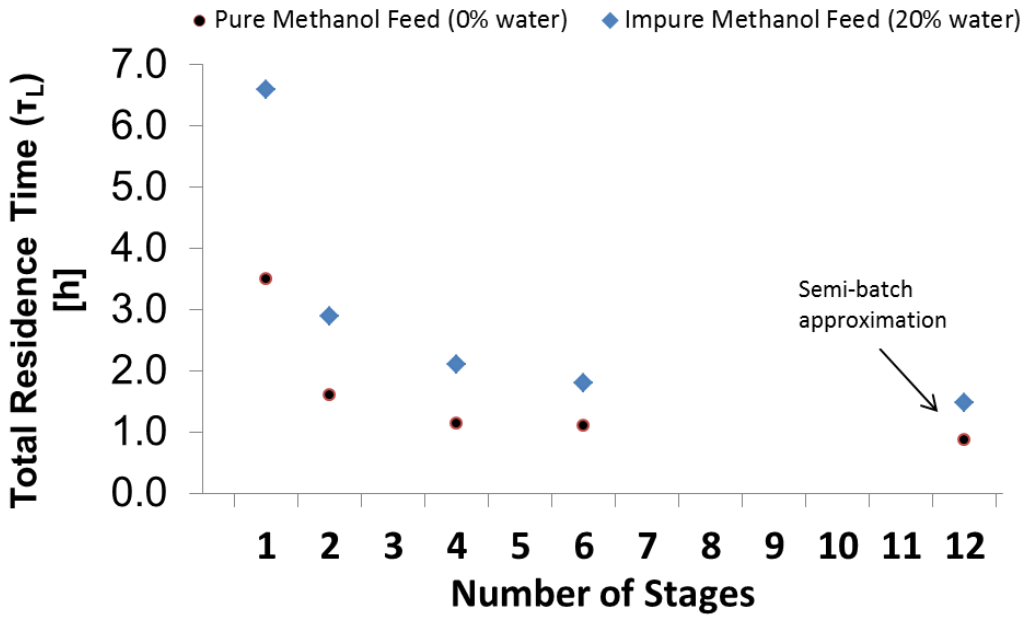

Figure 24: Effect of diminishing returns of number of stages on total residence time required to achieve >90% conversion in a continuous multistage bubble-column reactor operating at steady state

4.4.2. Effect of Methanol Vapor Feed Quality

Figure 25 shows the predictions of continuous bubble reactor model for pure and impure vapor feed containing 10 percent and 20 percent of water by volume in it. We can see that the model is able to capture the dilution effect as the continuous model predictions of overall conversion are lower than the semi-batch model predictions. We can also see that the overall conversion decreases for a particular reactor configuration as the water content increases in the vapor feed which again indicates that the continuous model is able to capture the kinetic equilibrium limitations on conversion due to presence of water in the system. Staging helps in preventing backmixing and improving reaction rate in each section. Although backmixing has been neglected in this case, but the model can successfully capture the improved reaction system from increase in staging. As the number of stages increase, the continuous reactor predictions are in more agreement with

the semi-batch reactor performance which indicates that the model can capture the positive effect of "staging" on overall conversion.

(a)

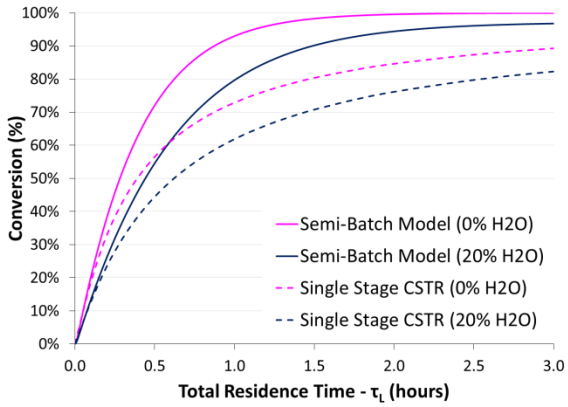

(b)

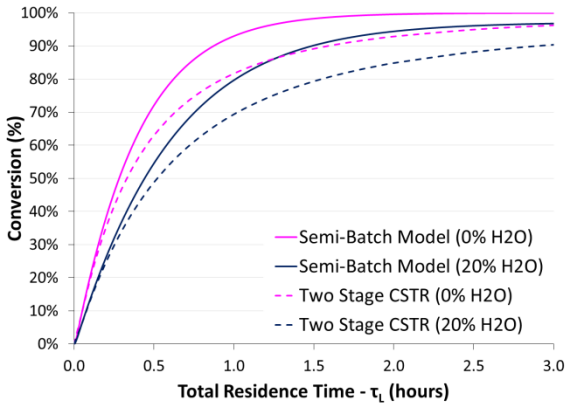

(c)

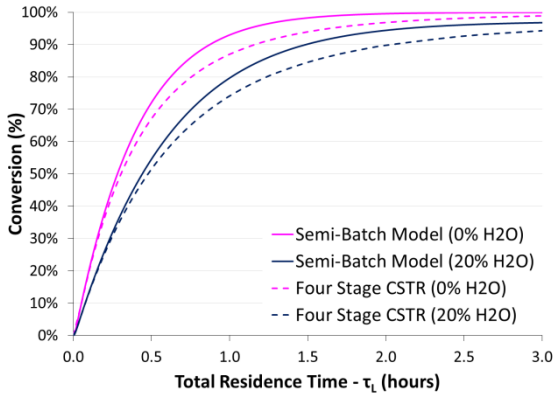

(d)

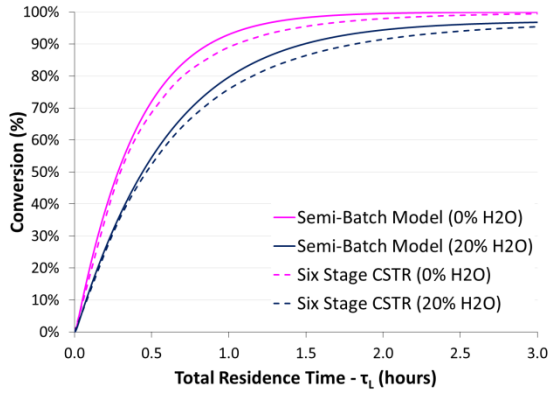

Figure 25: Model predictions for conversion profiles at different methanol vapor feed quality for semi-batch model and different steady state multistage configurations of bubble column reactor

5. Conclusion & Future Directions

5.1. Concluding Discussion

A mechanistic dynamic CSTR model was developed of a gas-liquid bubble column reactor to inspect its performance in semi-batch and continuous modes for biodiesel production via acid catalyzed esterification in presence of methanol. The reactor model formulated accounted for feed rates and residence times in both liquid and vapor phases, mass transfer of methanol and water across two phases, esterification kinetics of free fatty acids to fatty acid methyl esters and equilibrium limitations due to formation/presence of water in the system. The dynamic model consisted of several parameters which were estimated by non-linear regression analysis with semi-batch experimental data.

A low Damköhler number (Da = 0.03) was obtained from the non-linear regression analysis of the model for the best quality of fit with semi-batch data which indicated that the reactor operated in kinetics limited regime. The model could predict approximately 99% biodiesel conversion within 102 minutes (1.7 h) for pure methanol feed condition. Model predictions for conversion were approximately 98% and 97% within 150 minutes and 200 minutes of reaction time as water content in vapor feed was increased by 10% and 20% respectively. The model was able to capture the effect of water content in methanol vapor feed when compared to experimental results.

Parametric sensitivity study of the model conducted based on characteristic absorption time scale showed that there are three regimes which could exist in the reactor: (i) for Da<0.1, reactor performance is dominated by kinetics, (ii) for Da>2, reactor performance

is dominated by mass transfer and (iii) for 0.1<Da<2, reactor performance is dominated by effective result of competition between mass transfer and kinetics and showed that both mechanisms could co-exist in the reactor. There is a shift of regimes from more kinetic limited to more diffusion limited under this range of Damköhler number as the reaction progresses. Comparisons with methanol feed supply showed underestimation of conversion profile by the model which was attributed due to possible different catalyst concentration during the particular semi-batch conditions.

A steady state version of the semi-batch model was extended to a cross-flow multistage BCR model of *'n'* stages in continuous mode connected in series. Model predictions showed that for $n>6$, semi-batch reactor performance can be approximately achieved. An effect of diminishing returns was observed for concentration profiles as number of stages and cumulative residence time was increased. Also, effect of increasing water content in methanol feed on decreasing conversion was captured by the steady state CBCR model.

5.2. Future Directions

The reactor model developed in this thesis needs to be extended for accommodating transesterification and hydrolysis reactions. This is to make the model more comprehensive and complete in terms of predicting bubble column reactor performance when mixed feedstocks are used as raw materials for biodiesel production. A robust kinetic model should be built and incorporated in the main model to account for the different desired reactions (esterification and transesterification) and side reactions inside the reactor (saponification, hydrolysis).

Another immediate step to improve the model will be to re-derive the dynamic model and reduce the number of parameters which will make the curve fitting process more accurate and bounded. This will help in getting a better set of model parameters. The model could be extended by keeping the vapor-phase model in transient mode and avoid steady state. The curve fitting process could be made more effective via multiresponse parameter estimation by adjusting the parameters simultaneously comparing to both experiments conducted using 100 percent and 80 percent methanol vapor feed. Such a methodology for parameter estimation in kinetic modeling for iCVD of poly(alkyl acrylates) (*81*) has been employed.

More parametric experiments should be conducted to modify the current model parameters. Statistical methods could be used to build experimental designs at two or three factorial level by choosing important process variables that affects the biodiesel production. Response Surface Methodology (RSM) has been used for optimizing base catalyzed transesterification of rapeseed oil by studying the effect of temperature, reaction time and catalyst concentration according to a two level factorial design (*82*). This could be extended to acid catalyzed esterification and mixed feedstock biodiesel production process.

Bibliography

1. EIA Renewable Energy - U. S. Energy Consumption by Energy Source. http://www.eia.doe.gov/cneaf/alternate/page/renew_energy_consump/table1.html (accessed March 2011).

2. EIA Renewable Energy - Renewable Energy Consumption by Energy Use Sector and Energy Source. http://www.eia.doe.gov/cneaf/alternate/page/renew_energy_consump/table2.html (accessed March 2011).

3. Report: 12 billion gallons of biodiesel by 2020. *Biodiesel Magazine*, April 26, 2010.

4. Urbanchuk, J. M. *Contribution of the Biodiesel Industry to the Economy of the United States;* Prepared for the National Biodiesel Board; LECG, LLC, September 30, 2006.

5. Regulations & Standards | Fuels & Fuels Additives | US EPA, 2010. US Environmental Protection Agency. http://www.epa.gov/otaq/fuels/renewablefuels/regulations.htm (accessed March 2011).

6. Lane, J. Biodiesel revives! Senate passes tax credit extension; Imperium restarts production. http://biofuelsdigest.com/bdigest/2010/03/11/biodiesel-revives-senate-passes-tax-credit-extension-imperium-restarts-production/ (accessed March 2011).

7. Pahl, G.; McKibben, B. *Biodiesel: Growing a New Energy Economy*, 2nd ed.; Chelsea Green Publishing, 2008.

8. *A Comprehensive Analysis of Biodiesel Impacts on Exhaust Emissions;* Draft Technical Report; U.S. Environment Protection Agency, 2002.

9. Sheehan, J.; Camobreco, V.; Duffield, J.; Graboski, M.; Shapouri, H. *An Overview of Biodiesel and Petroleum Diesel Life Cycles;* Account of Work; U.S. Department of Commerce: Golden, CO, 1998.

10. Biodiesel Emissions. National Biodiesel Board - www.biodiesel.org - www.nbb.org. http://www.biodiesel.org/pdf_files/fuelfactsheets/emissions.pdf

(accessed March 01, 2011).

11. Sims, R.; Taylor, M.; Mabee, W. *From 1st to 2nd generation biofuel technologies - An overview of current industry and RD&D activities;* Full Report; International Energy Agency Bioenergy: Paris, November 2008.

12. Van Gerpen, J.; Shanks, B.; Pruszko, R.; Clements, D.; Knothe, G. *Biodiesel Production Technology;* Contractor Report; U.S. Department of Commerce, 2004.

13. Haas, M. J.; McAloon, A. J.; Yee, W. C.; Foglia, T. A. A process model to estimate biodiesel production costs. *Bioresource Technology* **2006,** *97* (4), 671-678.

14. Van Gerpen, J. Biodiesel processing and production. *Fuel Processing Technology* **2005,** *86* (10), 1097– 1107.

15. Meher, L. C.; Sagar, D. V.; Naik, S. N. Technical aspects of biodiesel production by transesterification—a review. *Renewable and Sustainable Energy Reviews* **2006,** *10* (3), 248-268.

16. Lang, X.; Dalai, A. K.; Bakhshi, N. N.; Reaney, M. J.; Hertz, P. B. Preparation and characterization of bio-diesels from various bio-oils. *Bioresource Technology* **2001,** *80* (1), 53-62.

17. Cairncross, R. A.; Mohammed, M.; Melick, C. A. Modeling of a Continuous Two-Phase Bubble Column Reactor for the Production of Biodiesel From Free Fatty Acids. *AIChE National Annual Meeting*, Nashville, 2009.

18. Noureddini, H.; Zhu, D. Kinetics of Transesterification of Soybean Oil. *Journal of the American Oil Chemists' Society* **1997,** *74* (11), 1457-1463.

19. Zhang, Y.; Dubé, M. A.; McLean, D. D.; Kates, M. Biodiesel production from waste cooking oil: 1. Process design and technological assessment. *Bioresource Technology* **2003,** *89* (1), 1-16.

20. Kulkarni, M. G.; Dalai, A. K. Waste Cooking Oil - An Economical Source for Biodiesel: A Review. *Catalysis and Chemical Reaction Engineering* **2006,** *45* (9), 2901–2913.

21. Wade, L. G. *Organic Chemistry,* 6th ed.; Prentice Hall, 2005.

22. Babcock, R. E.; Clausen, E. C.; Popp, M.; Schulte, W. B. Yield Characteristics of Biodiesel Produced from Chicken Fat-Tall Oil Blended Feedstocks. Mack-

Blackwell Rural Transportation Center Research Products. http://ww2.mackblackwell.org/web/research/ALL_RESEARCH_PROJECTS/2000s/2092/MBTC-2092.pdf.

23. Ghadge, S. V.; Raheman, H. Biodiesel production from mahua (Madhuca indica) oil having high free fatty acids. *Biomass and Bioenergy* **2005,** *28* (6), 601-605.

24. Zullaikah, S.; Lai, C.-C.; Vali, S. R.; Ju, Y.-H. A two-step acid-catalyzed process for the production of biodiesel from rice bran oil. *Bioresource Technology* **2005,** *96* (17), 1889-1896.

25. Ramadhas, A. S.; Jayaraj, S.; Muraleedharan, C. Biodiesel production from high FFA rubber seed oil. *Fuel* **2005,** *84* (4), 335-340.

26. Qiu, Z.; Zhao, L.; Weatherley, L. Process intensification technologies in continuous biodiesel production. *Chemical Engineering and Processing: Process Intensification* **2010,** *49* (4), 323-330.

27. Dias, J. M.; Alvim-Ferraz, M. C. M.; Almeida, M. F. Mixtures of Vegetable Oils and Animal Fat for Biodiesel Production: Influence on Product Composition and Quality. *Energy & Fuels* **2008,** *22* (6), 3889-3893.

28. Shahidi, F. *Bailey's Industrial Oil and Fat Products,* 6th ed.; John Wiley & Sons, 2005; Vol. 1, 6 vols..

29. Wahlen, B. D.; Barney, B. M.; Seefeldt, L. C. Synthesis of Biodiesel from Mixed Feedstocks and Longer Chain Alcohols Using an Acid-Catalyzed Method. *Energy Fuels* **2008,** *22* (6), 4223–4228.

30. Canakci, M.; Van Gerpen, J. Biodiesel production from oils and fats with high free fatty acids. **2001,** *44* (6), 1429-1436.

31. Potts, W.; Bolley, D. Analysis of the fruit of the Chinese Tallow tree in Texas. *Journal of the American Oil Chemists' Society* **1946,** *23* (10), 316-318.

32. Berrios, M.; Siles, J.; Martin, M. A.; Martin, A. A kinetic study of the esterification of free fatty acids (FFA) in sunflower oil. *Fuel* **2007,** *86* (15), 2383-2388.

33. Canoira, L.; Rodriguez-Gamero, M.; Querol, E.; Alcantara, R.; Lapuerta, M.; Oliva, F. Biodiesel from Low-Grade Animal Fat: Production Process Assessment and Biodiesel Properties Characterization. *Industrial & Engineering Chemistry Research* **2008,** *47* (21), 7997-8004.

34. Aranda, D. A.; Santos, R. T.; Tapanes, N. C.; Ramos, A. L.; Antunes, O. A. Acid-Catalyzed Homogeneous Esterification Reaction for Biodiesel Production from Palm Fatty Acids. *Catalysis Letters* **2007,** *122* (1), 20-25.

35. Alcantara, R.; Amores, J.; Canoira, L.; Fidalgo, E.; Franco , M. J.; Navarro, A. Catalytic production of biodiesel from soy-bean oil, used frying oil and tallow. *Biomass and Bioenergy* **2000,** *18* (6), 515-527.

36. Al-Zuhair, S.; Ling, F. W.; Jun, L. S. Proposed kinetic mechanism of the production of biodiesel from palm oil using lipase. *Process Biochemistry* **2007,** *42* (6), 951–960.

37. Al-Zuhair, S.; Dowaidar, A.; Kamal, H. Dynamic modeling of biodiesel production from simulated waste cooking oil using immobilized lipase. *Biochemical Engineering Journal* **2009,** *44* (2/3), 256-262.

38. Cheirsilp, B.; H-Kittikun, A.; Limkatanyu, S. Impact of transesterification mechanisms on the kinetic modeling of biodiesel production by immobilized lipase. *Biochemical Engineering Journal* **2008,** *42* (3), 261–269.

39. Kaieda, M.; Samukawa, T.; Matsumoto, T.; Ban, K.; Kondo, A.; Shimada, Y.; Noda, H.; Nomoto, F.; Ohtsuka, K.; Izumoto, E.; Fukuda, H. Biodiesel fuel production from plant oil catalyzed by Rhizopus oryzae lipase in a water-containing system without an organic solvent. *Journal of Bioscience and Bioengineering* **1999,** *88* (6), 627-631.

40. Shah, S.; Sharma, S.; Gupta, M. N. Biodiesel Preparation by Lipase-Catalyzed Biodiesel Preparation by Lipase-Catalyzed. *Energy & Fuels* **2004,** *18* (1), 154-159.

41. Park, J.-Y.; Wang, Z.-M.; Kim, D.-K.; Lee, J.-S. Effects of water on the esterification of free fatty acids by acid catalysts. *Renewable Energy* **2010,** *35* (3), 614-618.

42. Gryglewicz, S. Rapeseed oil methyl esters preparation using heterogeneous catalysts. *Bioresource Technology* **1999,** *70* (3), 249-253.

43. Cardoso, A. L.; Neves, S. C. G.; da Silva, M. J. Esterification of Oleic Acid for Biodiesel Production Catalyzed by SnCl2: A Kinetic Investigation. *Energies* **2008,** *1* (2), 79-92.

44. Hameed, B. H.; Lai, L. F.; Chin, L. H. Production of biodiesel from palm oil (Elaeis guineensis) using heterogeneous catalyst: An optimized process. *Fuel*

Processing Technology **2009,** *90* (4), 606-610.

45. Di Serio, M.; Ledda, M.; Cozzolino, M.; Minutillo, G.; Tesser, R.; Santacesaria, E. Transesterification of Soybean Oil to Biodiesel by Using Heterogeneous Basic Catalysts. *Industrial & Engineering Chemistry Research* **2006,** *45* (9), 3009–3014.

46. Suppes, G. J.; Dasari, M. A.; Doskocil, E. J.; Mankidy, P. J.; Goff, M. J. Transesterification of soybean oil with zeolite and metal catalysts. *Applied Catalysis A: General* **2004,** *257* (2), 213-223.

47. Marchetti, J. M.; Errazu, A. F. Comparison of different heterogeneous catalysts and different alcohols for the esterification reaction of oleic acid. *Fuel* **2008,** *87* (15-16), 3477-3480.

48. Mao, V.; Konar, S. K.; Boocock, D. G. B. The pseudo-single-phase, base-catalyzed transmethylation of soybean oil. *Journal of the American Oil Chemists' Society* **2004,** *81* (8), 803-808.

49. Dimian, A. C.; Omota, F.; Bliek, A. Entrainer-enhanced reactive distillation. *Chemical Engineering and Processing* **2004,** *43* (3), 411-420.

50. Omota, F.; Dimian, A. C.; Bliek, A. Fatty acid esterication by reactive distillation: Part 2—kinetics-based design for sulphated zirconia catalysts. *Chemical Engineering Science* **2003,** *58* (14), 3175-3185.

51. Omota, F.; Dimian, A. C.; Bliek, A. Fatty acid esterification by reactive distillation. Part 1: equilibrium-based design. *Chemical Engineering Science* **2003,** *58* (14), 3159-3174.

52. Kusdiana, D.; Saka, S. Effects of water on biodiesel fuel production by supercritical methanol treatment. *Bioresource Technology* **2003,** *91* (3), 289–295.

53. Glisic, S.; Skala, D. The problems in design and detailed analyses of energy consumption for biodiesel synthesis at supercritical conditions. *The Journal of Supercritical Fluids* **2009,** *49* (2), 293-301.

54. Vera, C. R.; D'Ippolito, S. A.; Pieck, C. L.; Parera, J. M. Production of biodiesel by a two-step supercritical reaction process with adsorption refining. *2nd Mercosur Congress on Chemical Engineering, 4th Mercosur Congress on Process Systems Engineering*, Rio de Janeiro, 2005.

55. Sun, P.; Wang, B.; Yao, J.; Zhang, L.; Xu, N. Fast Synthesis of Biodiesel at High

Throughput in Microstructured Reactors. *Industrial & Engineering Chemistry Research* **2009,** *49* (3), 1259–1264.

56. Sun, J.; Ju, J.; Ji, L.; Zhang, L.; Xu, N. Synthesis of Biodiesel in Capillary Microreactors. *Industrial & Engineering Chemistry Research* **2008,** *47* (5), 1398–1403.

57. Kocsisová, T.; Cvengros, J.; Lutisan, J. High-temperature esterification of fatty acids with methanol at ambient pressure. *European Journal of Lipid Science and Technology* **2005,** *107* (2), 87-92.

58. Joelianingsih; Hagiwara, S.; Nabetani, H.; Sagara, Y.; Soerawidjaya, T. H.; Tambunan, A. H.; Abdullah, K. Performance of a Bubble Column Reactor for the Non-Catalytic Methyl Esterification of Free Fatty Acids at Atmospheric Pressure. *Journal of Chemical Engineering of Japan* **2007,** *40* (9), 780-785.

59. Joelianingsih; Maeda, H.; Hagiwara, S.; Nabetani, H.; Sagara, Y.; Soerawidjaya, T. H.; Tambunan, A. H.; Abdullah, K. Biodiesel fuels from palm oil via the non-catalytic transesterification in a bubble column reactor at atmospheric pressure: A kinetic study. *Renewable Energy* **2008,** *33* (7), 1629-1636.

60. Mollenhauer, T.; Klemm, W.; Lauterbach, M.; Ondruschka, B.; Haupt, J. Process Engineering Study of the Homogenously Catalyzed Biodiesel Synthesis in a Bubble Column Reactor. *Industrial and Engineering Chemistry Research* **2010,** *49* (24), 12390–12398.

61. Hama, S.; Yamaji, H.; Fukumizu, T.; Numata, T.; Tamalampudi, S.; Kondo, A.; Noda, H.; Fukuda, H. Biodiesel-fuel production in a packed-bed reactor using lipase-producing Rhizopus oryzae cells immobilized within biomass support particles. *Biochemical Engineering Journal* **2007,** *34* (3), 273-278.

62. Suwannakarn, K.; Lotero, E.; Ngaosuwan, K.; Goodwin, Jr., J. G. Simultaneous Free Fatty Acid Esterification and Triglyceride Transesterification Using a Solid Acid Catalyst with in Situ Removal of Water and Unreacted Methanol. *Industrial & Engineering Chemistry Research* **2009,** *48* (6), 2810-2818.

63. Williams, R. pKa Values for Organic/Inorganic Acids, 2007. School of Chemistry at Pietermaritzburg. http://chemweb.unp.ac.za/chemistry/Physical_Data/pKa_values.htm (accessed March 01, 2011).

64. Rumack, B. H. *POISINDEX(R) Information System;* Brochure; Micromedex Inc.: Englewood, 2002. http://www.valdezhousing.com/inipol/pages/oleic.htm(accessed March 2011)

65. Kantarci, N.; Borak, F.; Ulgen, K. O. Bubble Column Reactors. *Process Biochemistry* **2005,** *40* (7), 2263-2283.

66. Jakobsen, H. A.; Lindborg, H.; Dorao, C. A. Modeling of Bubble Column Reactors: Progress and Limitations. *Industrial and Engineering Chemistry Research* **2005,** *44* (14), 5107–5151.

67. Darnoko, D.; Cheryan, M. Kinetics of palm oil transesterification in a batch reactor. *Journal of the American Oil Chemists' Society* **2000,** *77* (12), 1263-1267.

68. Freedman, B.; Pryde, E. H.; Mounts, T. L. Variables affecting the yields of fatty esters from transesterified vegetable oils. *Journal of the American Oil Chemists' Society* **1984,** *61* (10), 1638–1643.

69. Minami, E.; Saka, S. Kinetics of hydrolysis and methyl esterification for biodiesel production in two-step supercritical methanol process. *Fuel* **2006,** *85* (17-18), 2479–2483.

70. Stiefel, S.; Dassori, G. Simulation of Biodiesel Production through Transesterification of Vegetable Oils. *Industrial & Engineering Chemistry Research* **2008,** *48* (3), 1068-1071.

71. Mjalli, F. S.; San, L. K.; Yin, K. C.; Hussain, M. A. Dynamics and Control of a Biodiesel Transesterification Reactor. *Chemical Engineering & Technology* **2009,** *32* (1), 13–26.

72. Slinn, M.; Kendall, K. Developing the reaction kinetics for a biodiesel reactor. *Bioresource Technology* **2009,** *100* (7), 2324-2327.

73. Melick, C. A. *Studies for Bubble Column Design to Produce BioDiesel;* Research; Unpublished: Philadelphia, 2008.

74. Ruiz, A.; Serina, M.; Temple, J.; Vena, N.; Wilson, B. *A Novel Reactor Design for Efficient Production of Biodiesel from High Free-Fatty-Acid Oils;* Senior Design Report; Unpublished: Philadelphia, 2008.

75. Falch, E. A.; Gaden Jr, E. L. A continuous, multistage tower fermentor. I. Design and performance tests. *Biotechnology and Bioengineering* **1969,** *11* (5), 927–943.

76. Khare, A. S.; Dharwadkar, S. V.; Joshi, J. B.; Sharma, M. Liquid- and Solid-Phase Mixing in a Sectionalized Bubble Column Slurry Reactor. *Industrial & Engineering Chemistry Research* **1990,** *29* (7), 1503–1509.

77. John, N.; Nicosia, K.; Petragnani, M.; Schwartzbach, B.; Wilrigs, S. *Novel Reactor Design for Biodiesel Production;* Senior Design Report (Team MEM - 19); Unpublished: Philadelphia, 2009.

78. Lotero, E.; Liu, Y.; Lopez, D. E.; Suwannakarn, K.; Bruce, D. A.; Goodwin, Jr., J. G. Synthesis of Biodiesel via Acid Catalysis. *Industrial and Engineering Chemistry Research* **2005,** *44* (14), 5353–5363.

79. Chen, F.; Huss, R. S.; Doherty, M. F.; Malone, M. F. Multiple steady states in reactive distillation: kinetic effects. *Computers & Chemical Engineering* **2002,** *26* (1), 81-93.

80. Deen, W. M. *Analysis of Transport Phenomena (Topics in Chemical Engineering),* 1st ed.; Oxford University Press: New York USA, 1998.

81. Lau, K. K. S.; Gleason, K. Initiated Chemical Vapor Deposition (iCVD) of Poly(alkyl acrylates): A Kinetic Model. *Macromolecules* **2006,** *39* (10), 3695-3703.

82. Ferella, F.; Di Celso, G. M.; Michelis, I. D.; Stanisci, V.; Vegliò, F. Optimization of the transesterification reaction in biodiesel production. *Fuel* **2010,** *89* (1), 36-42.

83. Shorter, J. A.; De Bruyn, W. J.; Hu, J.; Swartz, E.; Davidovits, P.; Worsnop, D. R.; Zahniser, M. S.; Kolb, C. E. Bubble Column Apparatus for Gas-Liquid Heterogeneous Chemistry Studies. *Environmental Science & Technology* **1995,** *29* (5), 1171–1178.

84. Bird, R. B.; Stewart, W. E.; Lightfoot, E. N. *Transport Phenomena,* 2nd ed.; John Wiley & Sons, Inc.: New York, 2002.

85. Haas, F. M.; Sanchez, J.; Letterle, K. *Design of a Waste Cooking Oil Upgrader for BioFuel Processing: Trap Grease Pretreatment;* Senior Design Report; Unpublished: Philadelphia, 2005.